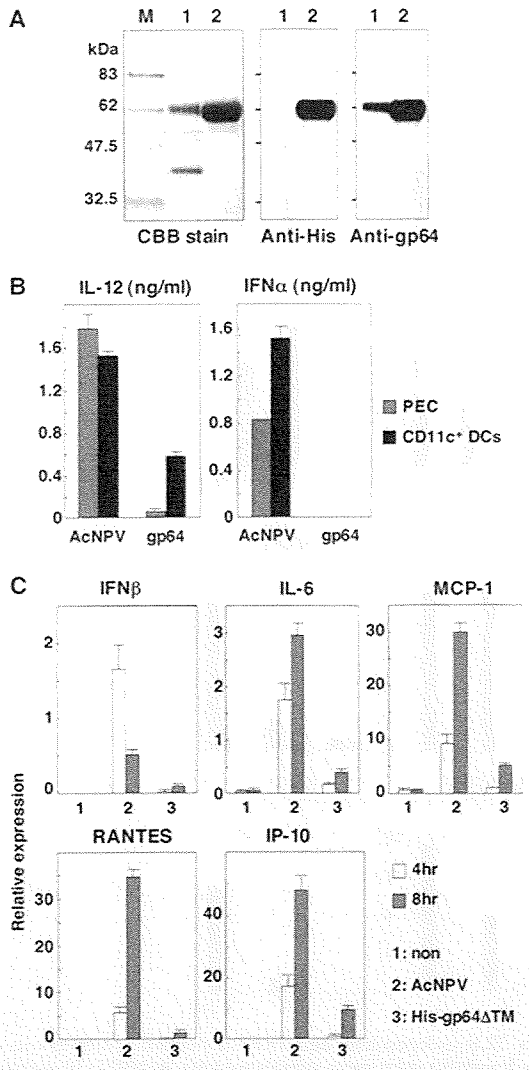

FIG. 4. Immune activation by AcNPV is not mediated by gp64. (A) His-gp64ΔTM expressed in Sf-9 cells was purified and subjected to sodium dodecyl sulfate-12.5% polyacrylamide gel electrophoresis under reducing conditions. Molecular size markers (lane M), purified AcNPV particles (lanes 1), and His-gp64ΔTM (lanes 2) were visualized by Coomassie blue (CBB) staining (left) and immunoblotting using antihexahistidine monoclonal antibody (middle) and anti-gp64 antibody (AcV5) (right). (B) PECs and splenic $CD11c^+$ DCs (2×10^5 cells/well) prepared from wild-type mice were stimulated with AcNPV (10 μg/ml) or His-gp64ΔTM (gp64) (20 μg/ml). After 24 h of incubation, production of IL-12 and IFN-α in culture supernatants was determined by ELISA. (C) MEFs (3×10^5 cells/well) prepared from wild-type mice were stimulated with AcNPV (10 μg/ml) or His-gp64ΔTM (20 μg/ml). At 4 h or 8 h poststimulation, total RNA was extracted and expression of mRNA of IFN-β, IL-6, MCP-1, RANTES, and IP-10 was determined by real-time PCR. Data are shown as the means ± standard deviations.

vation by AcNPV in MEFs, wild-type MEFs were pretreated with AcNPV or poly(I:C) and challenged with VSV (GLPLF mutant). Pretreatment with AcNPV (0.016 μg/ml to 2 μg/ml) or poly(I:C) (0.2 μg/ml to 25 μg/ml) conferred antiviral status against VSV infection in MEFs in a dose-dependent manner (Fig. 6C, left, and E). However, the induction of antiviral status by AcNPV or poly(I:C) treatment was completely abrogated in IRF3-deficient MEFs (Fig. 6C, right). On the other hand, pretreatment with IFN-α (10^1 to 10^4 U/ml) conferred antiviral status against VSV infection in both IRF knockout MEFs in a dose-dependent manner (Fig. 6D). These results clearly indicate that IRF3 plays a crucial role in the induction of antiviral status in MEFs by AcNPV.

Involvement of a TLR- and RIG-I/IPS-1-independent signaling pathway in immune activation by AcNPV. TLR3 has been shown to recognize viral dsRNA as well as a synthetic dsRNA analogue, poly(I:C), in the intracellular compartment. Recently, RIG-I and MDA5 have been identified as TLR-independent cytoplasmic RNA detectors and shown to induce type I IFN production through an adaptor molecule, IPS-1, that localizes in mitochondria (26, 36, 42, 47). To examine the involvement of TLR-independent cytoplasmic DNA-sensing machinery in the immune activation by AcNPV, as seen in the recognition of intracellular RNA, the production of type I IFN and IFN-inducible chemokines in PECs and splenic $CD11c^+$ DCs derived from RIG-I-, MDA5-, or IPS-1-deficient mice was examined. Type I IFN production in PECs and splenic $CD11c^+$ DCs in response to VSV and poly(I:C) was impaired by knockout of IPS-1, whereas AcNPV produced a significant amount of the IFNs in the IPS-1 knockout immune cells (Fig. 7A). Furthermore, IFN production in the immune cells in response to VSV was abrogated by knockout of the RIG-I gene but not by knockout of the MDA5 gene; however, AcNPV produced significant amounts of the IFNs in the RIG-I or MDA5 knockout immune cells (data not shown).

Next, to determine whether IPS-1 is involved in the production of type I IFN and IFN-inducible chemokines in MEFs in response to AcNPV, production of the cytokines in the IPS-1-deficient MEFs in response to VSV or AcNPV was examined (Fig. 7B). Production of IFN-β, IL-6, MCP-1, RANTES, and IP-10 was severely impaired in IPS-1-deficient MEFs upon VSV infection, whereas AcNPV produced substantial amounts of the cytokines in the IPS-1-deficient MEFs in spite of a slight reduction in IFN-β and IL-6 production (Fig. 7B). Similarly, production of the IFN-inducible chemokines in MEFs infected with VSV, but not with AcNPV, was also severely impaired by knockout of the RIG-I gene (data not shown). Collectively, these results suggest that a novel TLR- and RIG-I/IPS-1-independent signaling pathway(s) participated in the production of type I IFN and the IFN-inducible chemokines in both immunocompetent cells and MEFs in response to AcNPV infection.

DISCUSSION

Recent progress has been made in the identification of receptors, signal transduction molecules, and transcription factors that are required for the induction of type I IFN in cells upon infection with RNA and DNA viruses, as well as for the robust IFN production in pDCs, suggesting the presence of multiple signaling pathways for type I IFN induction (17, 23, 25). Production of type I IFN was shown to be induced through a number of different pathways in a cell-type-specific manner upon infection with HSV (40), although the precise mechanisms involved in sensing the foreign DNA of microorganisms remain largely unknown. In this study, we have examined the molecular mechanisms of type I IFN induction by AcNPV infection both in professional immune cells, including pDCs,

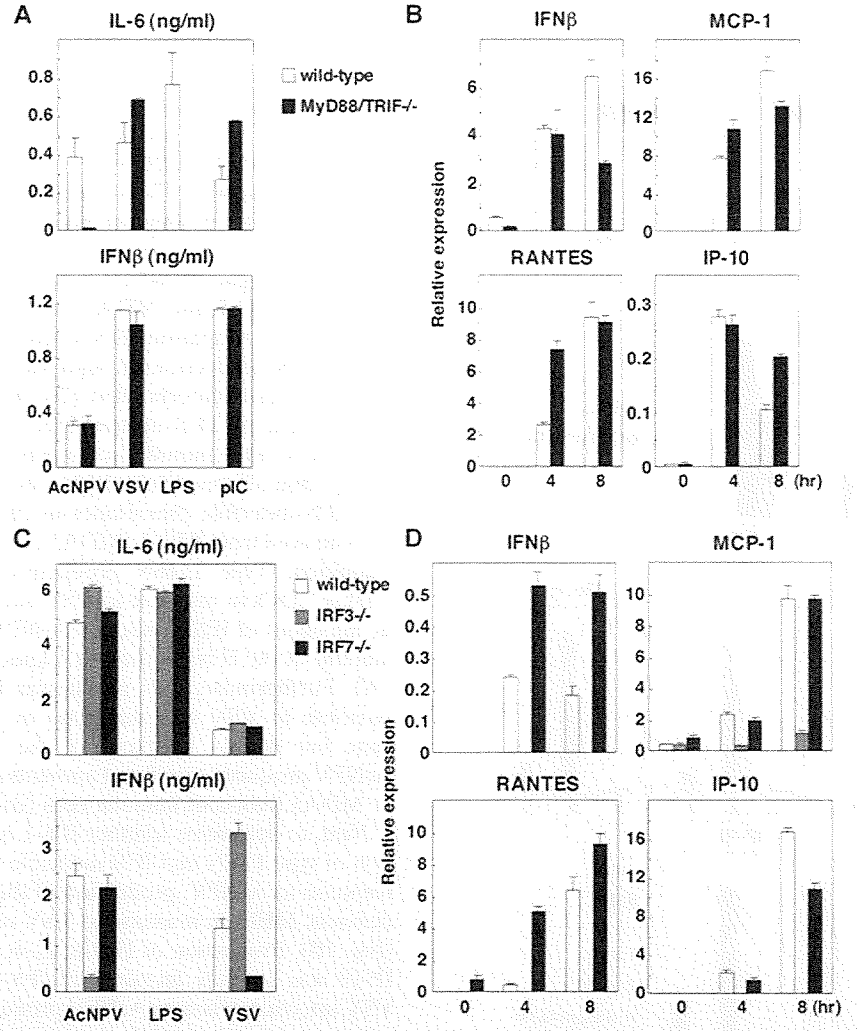

FIG. 5. AcNPV produces IFN-β and IFN-inducible chemokines through a TLR-independent and IRF3-dependent pathways in MEFs. (A) MEFs (2×10^4 cells/well) prepared from wild-type or MyD88/TRIF double knockout mice were stimulated with AcNPV (10 μg/ml), VSV (NCP mutant, MOI of 0.1), LPS (10 μg/ml), or poly(I:C) (pIC) (50 μg/ml). After 24 h of incubation, production of IL-6 and IFN-β in culture supernatants was determined by ELISA. (B) MEFs (3×10^5 cells/well) prepared from wild-type or MyD88/TRIF double knockout mice were stimulated with AcNPV (10 μg/ml). Total RNA was extracted at the indicated time points, and the expression of mRNA of IFN-β, MCP-1, RANTES, and IP-10 was determined by real-time PCR. (C) MEFs (2×10^4 cells/well) prepared from wild-type, IRF3-deficient, or IRF7-deficient mice were stimulated with AcNPV (10 μg/ml), LPS (10 μg/ml), or VSV (NCP mutant, MOI of 0.1). After 24 h of incubation, the production of IL-6 and IFN-β in culture supernatants was determined by ELISA. (D) MEFs (3×10^5 cells/well) prepared from wild-type, IRF3-deficient, or IRF7-deficient mice were stimulated with AcNPV (10 μg/ml). Total RNA was extracted at the indicated time points, and the expression of mRNA of IFN-β, MCP-1, RANTES, and IP-10 was determined by real-time PCR. Data are shown as the means ± standard deviations.

PECs, and splenic $CD11c^+$ DCs, and in nonimmune cells and raised the possibility of the involvement of a novel TLR- and IPS-1-independent pathway in the production of type I IFN in vitro as well as in vivo in response to AcNPV infection.

The frequency of bioactive CpG motifs capable of inducing immune activation through a TLR9-dependent pathway in the AcNPV genome was similar to that in *E. coli* and HSV and was significantly higher than that in entomopoxvirus (1, 51). Furthermore, it was shown that HSV and murine cytomegalovirus produce inflammatory cytokines and type I IFN through both TLR9-dependent and -independent pathways (7, 15, 29, 32, 44). Recently, it was also reported that adenovirus DNA produced IL-6 and IFN-α through an entirely TLR/MyD88-independent pathway in non-pDCs (53), although the presence of the CpG motifs in the adenoviral genome has not yet been determined. The current model of TLR9 activation by viral DNA is as follows. The virus particles are internalized into cells and degraded within the endocytic vesicles, and the digested viral genome subsequently actives TLR9 localized in the endosomal compartments. Treatment with inhibitors for endosomal maturation or acidification efficiently inhibits TLR7 and TLR9 activation by viral RNA and DNA, respectively (8, 32, 33). Interestingly, the production of type I IFN in PECs upon infection with AcNPV was resistant to pretreatment with endocytosis inhibitors, suggesting that the cytoplasmic recognition of AcNPV by TLR-independent immune sensors may be required for type I IFN production in PECs. The purified AcNPV DNA encapsulated in liposomes induced the produc-

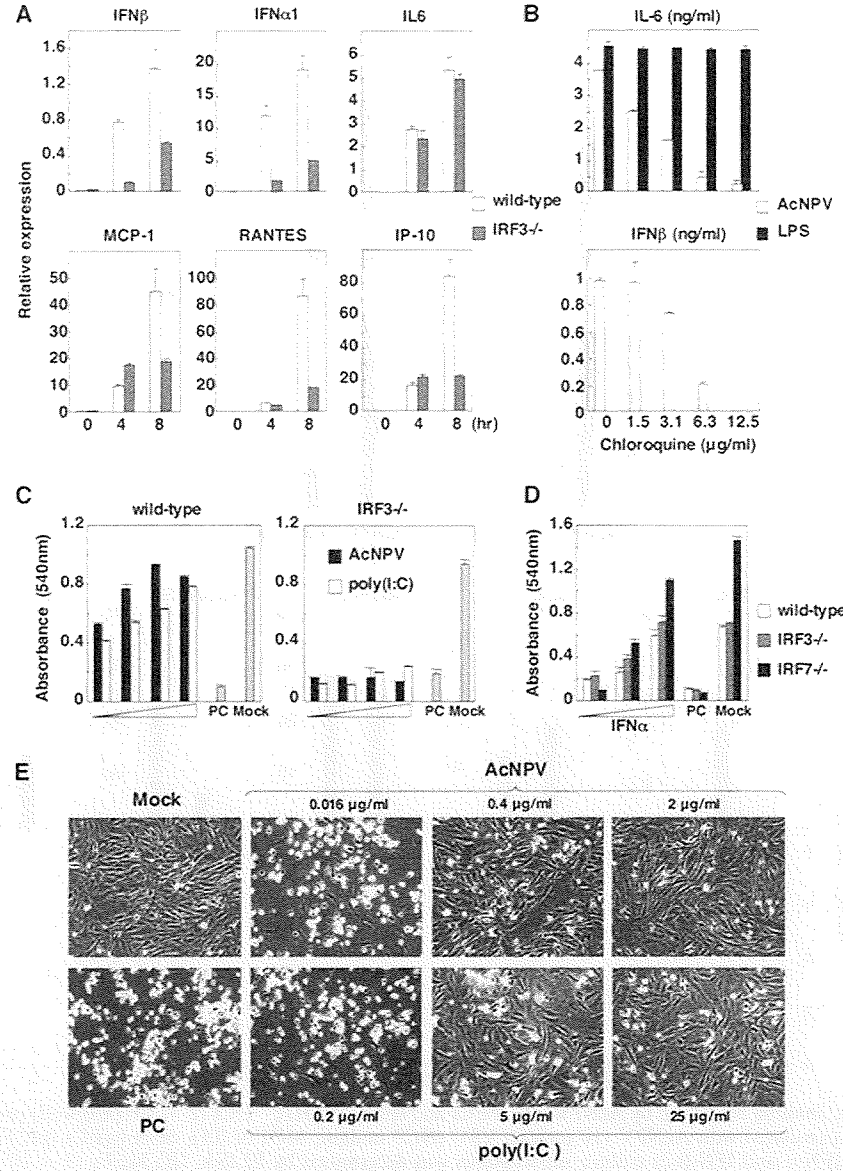

FIG. 6. AcNPV induces antiviral status in MEFs through an IRF3-dependent pathway. (A) MEFs (3×10^5 cells/well) prepared from wild-type and IRF3-deficient mice were transfected with AcNPV DNA (25 μg/ml). Total RNA was extracted at the indicated time points, and the expression of mRNA of IFN-β, IFN-α1, MCP-1, RANTES, IL-6, and IP-10 was determined by real-time PCR. (B) MEFs (2×10^4 cells/well) prepared from wild-type mice were stimulated with AcNPV (10 μg/ml) or LPS (10 μg/ml) in the presence of the indicated concentrations of chloroquine. After 24 h of incubation, production of IL-6 and IFN-β in culture supernatants was determined by ELISA. (C) MEFs (2×10^4 cells/well) prepared from wild-type and IRF3-deficient mice were incubated with AcNPV (0.016 μg/ml to 2 μg/ml) or poly(I:C) (0.2 μg/ml to 25 μg/ml). After 24 h of incubation, cells were washed extensively with warm medium and infected with VSV (GLPLF mutant, MOI of 0.1). Cell viability was determined at 24 h postinfection by crystal violet staining and quantitated by spectroscopy. (D) MEFs (2×10^4 cells/well) prepared from wild-type, IRF3-deficient, or IRF7-deficient mice were incubated with serial dilutions of murine IFN-α (10^1 to 10^4 U/ml). After 24 h of incubation, cells were washed extensively with warm medium and infected with VSV (GLPLF strain, MOI of 0.1). Cell viability was determined at 24 h postinfection by crystal violet staining and quantitated by spectroscopy. Values are plotted as means from the triplicate wells. Data are shown as means ± standard deviations. (E) Microscopic observation of MEFs from wild-type mice, showing the antiviral status against VSV infection by the treatment with AcNPV or poly(I:C) in a dose-dependent manner. PC, infected cells; Mock, mock-infected cells. Samples are shown at a magnification of ×40.

tion of type I IFN through both TLR9/MyD88-dependent and -independent pathways in PECs. These results indicate that the genomic DNA of AcNPV is recognized by at least two different pathways, TLR9-dependent endosomal recognition and TLR9-independent cytoplasmic recognition, and that type I IFN production by AcNPV is totally dependent on the latter process. However, the precise mechanisms of the immune activation of immunocompetent cells by AcNPV DNA through a TLR-independent pathway remain unknown. Therefore, further studies are needed to determine the molecular mechanisms underlying the type I IFN production through a TLR-independent cytoplasmic sensor for baculovirus DNA.

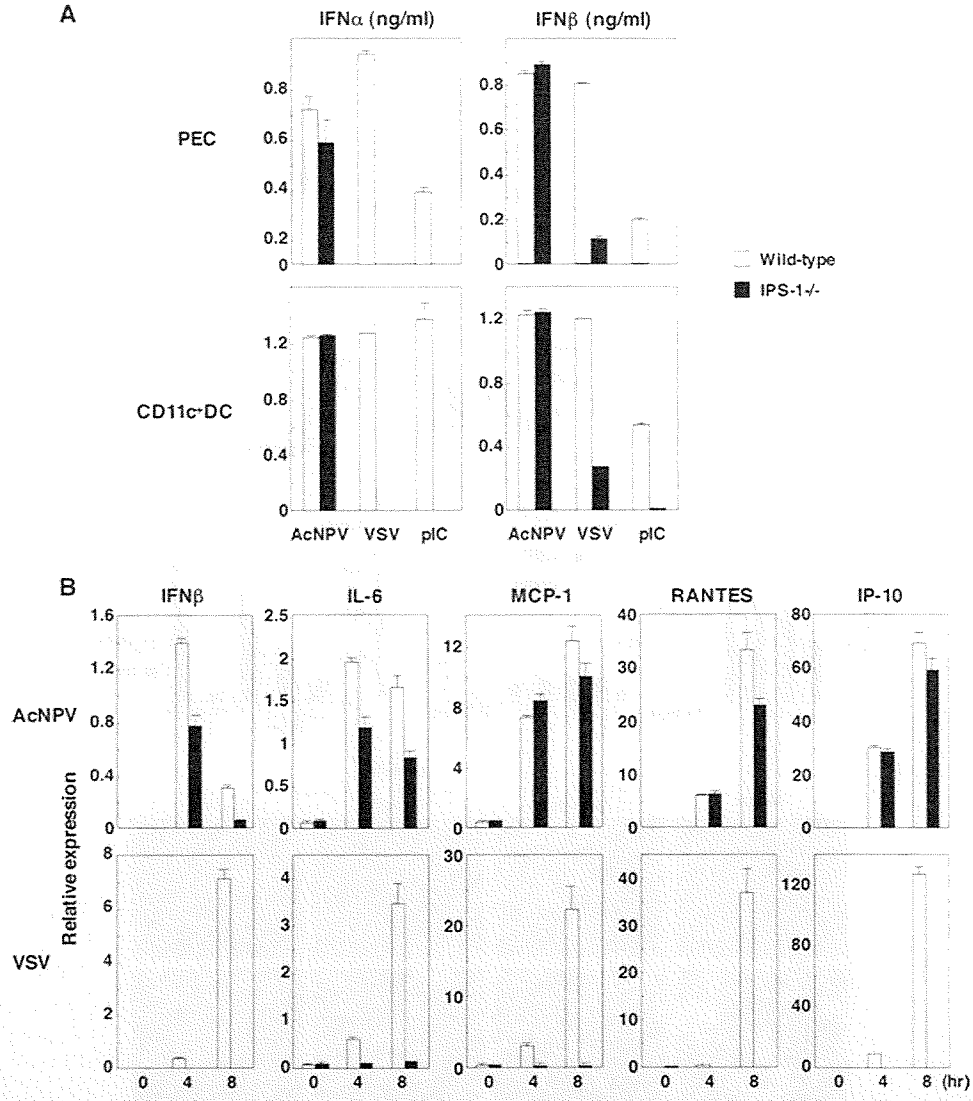

FIG. 7. Role of IPS-1 in immune activation by AcNPV. (A) PECs and splenic CD11c$^+$ DCs (2×10^5 cells/well) prepared from wild-type and IPS-1-deficient mice were stimulated with AcNPV (10 μg/ml), VSV (NCP mutant, MOI of 0.1), or poly(I:C) (pIC) (50 μg/ml). After 24 h of incubation, production of IFN-α and IFN-β in culture supernatants was determined by ELISA. (B) MEFs (3×10^5 cells/well) prepared from wild-type and IPS-1-deficient mice were stimulated with AcNPV (10 μg/ml) or VSV (NCP mutant, MOI of 0.1). Total RNA was extracted at the indicated time points, and the expression of mRNA of IFN-β, MCP-1, RANTES, IL-6, and IP-10 was determined by real-time PCR. Data are shown as the means ± standard deviations.

A novel TLR-independent cytosolic surveillance system for transfected dsDNA that elicits type I IFN induction through a TANK binding kinase 1 (TBK1)/IκB kinase-related kinase (IKKi)/IRF3 pathway has been shown to exist (19, 43). Our preliminary data also indicate that type I IFN production was severely reduced in TBK1-deficient MEFs in response to AcNPV and insufficient to protect cells from VSV infection (data not shown), suggesting the involvement of TBK1 in AcNPV-induced immune activation. Recently, a cytoplasmic recognition receptor, DAI (DNA-dependent activator of IRFs), was shown to be activated by dsDNA from a variety of sources and to produce type I IFN through an IRF3 and probably IRF7 pathway (45). However, there are conflicting reports suggesting a lack of impairment of type I IFN production in DAI knockout mice and DAI knockdown murine macrophages or MEFs in response to dsDNA of synthetic B-form DNA and from bacteria (4, 20). In this study, we have shown that splenic CD11c$^+$ DCs derived from IRF3-deficient mice produced a level of type I IFN compatible with that in wild-type mice in response to AcNPV, in contrast to the lack of IFN-β production in the PECs derived from the IRF3-deficient mice. More recently, two groups reported the identification of a membrane protein, termed mitochondrial mediator of IRF3 activation (MITA) or stimulator of IFN genes (STING), that activates IRF3 to induce a type I IFN response to viral infection (21, 52). Although both groups described slightly different characterizations of MITA, or STING, in terms of localization and signal transduction, both groups exhibited the opinion that MITA or STING plays a critical role in type I IFN production by B-form DNA. Although DAI-mediated type I IFN production was more

dependent on IRF3 than on IRF7, the cytoplasmic DNA sensors, including DAI and MITA or STING, may participate in the induction of type I IFN upon infection with AcNPV.

In the cytoplasm, RIG-I and MDA5 are critically involved in the recognition of dsRNA, and the adaptor molecule IPS-1 interacts with RIG-I and MDA5 to facilitate TBK1- and IKKi-mediated IRF3 and IRF7 activation, which leads to termination of the replication of RNA viruses through the helicase function. In addition, RIG-I has been shown to discriminate viral RNAs from the vast number and variety of cellular RNAs by recognizing a terminal 5′ triphosphate, but not 5′ OH or a 5′ methylguanosine cap (37, 39). In this study, both RIG-I- and IPS-1-deficient MEFs but not immunocompetent cells partially impaired the production of IFN-β and IL-6, but not that of MCP-1, RANTES, and IP-10, in response to AcNPV, suggesting the possible generation of dsRNA in MEFs upon infection with AcNPV in spite of the lack of replication. Although there is no evidence for the functional expression of the viral proteins, transcription of immediate-early genes of baculovirus was detected in HeLa and BHK cells upon infection with AcNPV by DNA microarray analysis (10) and in HEK293 cells and rat primary Schwann cells upon infection with *Bombyx mori* NPV by reverse transcription-PCR (27). These reports are consistent with our observations that the RIG-I/IPS-1 pathway partially participates in type I IFN induction by AcNPV infection in MEFs.

We have shown previously that an intranasal inoculation of AcNPV induces protective immunity from a lethal challenge of influenza A virus in mice (2) and that AcNPV produces type I IFN in immune cells of mice via a TLR9/MyD88-independent pathway (1). Our present studies further confirmed that AcNPV induces a strong antiviral immunity through a TLR-independent pathway. Although further studies are needed to clarify the precise mechanisms underlying the antiviral responses, a TLR-independent and probably TBK1-IRF3/IRF7-dependent signaling pathway may contribute to the induction of protective immunity against viral challenge induced by AcNPV infection in vivo.

ACKNOWLEDGMENTS

We thank H. Murase for her secretarial work.

This work was supported in part by grants-in-aid from the Research and Development Program for New Bio-industry Initiatives of Bio-oriented Technology Research Advancement Institution (BRAIN) and the Ministry of Education, Culture, Sports, Science, and Technology, Japan.

We have no conflicting financial interests.

REFERENCES

1. **Abe, T., H. Hemmi, H. Miyamoto, K. Moriishi, S. Tamura, H. Takaku, S. Akira, and Y. Matsuura.** 2005. Involvement of the Toll-like receptor 9 signaling pathway in the induction of innate immunity by baculovirus. J. Virol. **79**:2847–2858.
2. **Abe, T., H. Takahashi, H. Hamazaki, N. Miyano-Kurosaki, Y. Matsuura, and H. Takaku.** 2003. Baculovirus induces an innate immune response and confers protection from lethal influenza virus infection in mice. J. Immunol. **171**:1133–1139.
3. **Bjorck, P.** 2001. Isolation and characterization of plasmacytoid dendritic cells from Flt3 ligand and granulocyte-macrophage colony-stimulating factor-treated mice. Blood **98**:3520–3526.
4. **Charrel-Dennis, M., E. Latz, K. A. Halmen, P. Trieu-Cuot, K. A. Fitzgerald, D. L. Kasper, and D. T. Golenbock.** 2008. TLR-independent type I interferon induction in response to an extracellular bacterial pathogen via intracellular recognition of its DNA. Cell Host Microbe **4**:543–554.
5. **Chessler, A. D., L. R. Ferreira, T. H. Chang, K. A. Fitzgerald, and B. A. Burleigh.** 2008. A novel IFN regulatory factor 3-dependent pathway activated by trypanosomes triggers IFN-beta in macrophages and fibroblasts. J. Immunol. **181**:7917–7924.
6. **Coccia, E. M., M. Severa, E. Giacomini, D. Monneron, M. E. Remoli, I. Julkunen, M. Cella, R. Lande, and G. Uze.** 2004. Viral infection and Toll-like receptor agonists induce a differential expression of type I and lambda interferons in human plasmacytoid and monocyte-derived dendritic cells. Eur. J. Immunol. **34**:796–805.
7. **Delale, T., A. Paquin, C. Asselin-Paturel, M. Dalod, G. Brizard, E. E. Bates, P. Kastner, S. Chan, S. Akira, A. Vicari, C. A. Biron, G. Trinchieri, and F. Briere.** 2005. MyD88-dependent and -independent murine cytomegalovirus sensing for IFN-alpha release and initiation of immune responses in vivo. J. Immunol. **175**:6723–6732.
8. **Diebold, S. S., T. Kaisho, H. Hemmi, S. Akira, and C. Reis e Sousa.** 2004. Innate antiviral responses by means of TLR7-mediated recognition of single-stranded RNA. Science **303**:1529–1531.
9. **Diebold, S. S., M. Montoya, H. Unger, L. Alexopoulou, P. Roy, L. E. Haswell, A. Al-Shamkhani, R. Flavell, P. Borrow, and C. Reis e Sousa.** 2003. Viral infection switches non-plasmacytoid dendritic cells into high interferon producers. Nature **424**:324–328.
10. **Fujita, R., T. Matsuyama, J. Yamagishi, K. Sahara, S. Asano, and H. Bando.** 2006. Expression of *Autographa californica* multiple nucleopolyhedrovirus genes in mammalian cells and upregulation of the host beta-actin gene. J. Virol. **80**:2390–2395.
11. **Gilliet, M., W. Cao, and Y. J. Liu.** 2008. Plasmacytoid dendritic cells: sensing nucleic acids in viral infection and autoimmune diseases. Nat. Rev. Immunol. **8**:594–606.
12. **Gronowski, A. M., D. M. Hilbert, K. C. Sheehan, G. Garotta, and R. D. Schreiber.** 1999. Baculovirus stimulates antiviral effects in mammalian cells. J. Virol. **73**:9944–9951.
13. **Hemmi, H., O. Takeuchi, T. Kawai, T. Kaisho, S. Sato, H. Sanjo, M. Matsumoto, K. Hoshino, H. Wagner, K. Takeda, and S. Akira.** 2000. A Toll-like receptor recognizes bacterial DNA. Nature **408**:740–745.
14. **Hervas-Stubbs, S., P. Rueda, L. Lopez, and C. Leclerc.** 2007. Insect baculoviruses strongly potentiate adaptive immune responses by inducing type I IFN. J. Immunol. **178**:2361–2369.
15. **Hochrein, H., B. Schlatter, M. O'Keeffe, C. Wagner, F. Schmitz, M. Schiemann, S. Bauer, M. Suter, and H. Wagner.** 2004. Herpes simplex virus type-1 induces IFN-alpha production via Toll-like receptor 9-dependent and -independent pathways. Proc. Natl. Acad. Sci. USA **101**:11416–11421.
16. **Honda, K., and T. Taniguchi.** 2006. IRFs: master regulators of signalling by Toll-like receptors and cytosolic pattern-recognition receptors. Nat. Rev. Immunol. **6**:644–658.
17. **Honda, K., H. Yanai, T. Mizutani, H. Negishi, N. Shimada, N. Suzuki, Y. Ohba, A. Takaoka, W. C. Yeh, and T. Taniguchi.** 2004. Role of a transductional-transcriptional processor complex involving MyD88 and IRF-7 in Toll-like receptor signaling. Proc. Natl. Acad. Sci. USA **101**:15416–15421.
18. **Honda, K., H. Yanai, H. Negishi, M. Asagiri, M. Sato, T. Mizutani, N. Shimada, Y. Ohba, A. Takaoka, N. Yoshida, and T. Taniguchi.** 2005. IRF-7 is the master regulator of type-I interferon-dependent immune responses. Nature **434**:772–777.
19. **Ishii, K. J., C. Coban, H. Kato, K. Takahashi, Y. Torii, F. Takeshita, H. Ludwig, G. Sutter, K. Suzuki, H. Hemmi, S. Sato, M. Yamamoto, S. Uematsu, T. Kawai, O. Takeuchi, and S. Akira.** 2006. A Toll-like receptor-independent antiviral response induced by double-stranded B-form DNA. Nat. Immunol. **7**:40–48.
20. **Ishii, K. J., T. Kawagoe, S. Koyama, K. Matsui, H. Kumar, T. Kawai, S. Uematsu, O. Takeuchi, F. Takeshita, C. Coban, and S. Akira.** 2008. TANK-binding kinase-1 delineates innate and adaptive immune responses to DNA vaccines. Nature **451**:725–729.
21. **Ishikawa, H., and G. N. Barber.** 2008. STING is an endoplasmic reticulum adaptor that facilitates innate immune signalling. Nature **455**:674–678.
22. **Jayakar, H. R., and M. A. Whitt.** 2002. Identification of two additional translation products from the matrix (M) gene that contribute to vesicular stomatitis virus cytopathology. J. Virol. **76**:8011–8018.
23. **Kato, H., S. Sato, M. Yoneyama, M. Yamamoto, S. Uematsu, K. Matsui, T. Tsujimura, K. Takeda, T. Fujita, O. Takeuchi, and S. Akira.** 2005. Cell type-specific involvement of RIG-I in antiviral response. Immunity **23**:19–28.
24. **Kawai, T., and S. Akira.** 2006. Innate immune recognition of viral infection. Nat. Immunol. **7**:131–137.
25. **Kawai, T., S. Sato, K. J. Ishii, C. Coban, H. Hemmi, M. Yamamoto, K. Terai, M. Matsuda, J. Inoue, S. Uematsu, O. Takeuchi, and S. Akira.** 2004. Interferon-alpha induction through Toll-like receptors involves a direct interaction of IRF7 with MyD88 and TRAF6. Nat. Immunol. **5**:1061–1068.
26. **Kawai, T., K. Takahashi, S. Sato, C. Coban, H. Kumar, H. Kato, K. J. Ishii, O. Takeuchi, and S. Akira.** 2005. IPS-1, an adaptor triggering RIG-I- and Mda5-mediated type I interferon induction. Nat. Immunol. **6**:981–988.
27. **Kenoutis, C., R. C. Efrose, L. Swevers, A. A. Lavdas, M. Gaitanou, R. Matsas, and K. Iatrou.** 2006. Baculovirus-mediated gene delivery into mammalian cells does not alter their transcriptional and differentiating potential but is accompanied by early viral gene expression. J. Virol. **80**:4135–4146.
28. **Kost, T. A., J. P. Condreay, and D. L. Jarvis.** 2005. Baculovirus as versatile

vectors for protein expression in insect and mammalian cells. Nat. Biotechnol. **23**:567–575.
29. **Krug, A., G. D. Luker, W. Barchet, D. A. Leib, S. Akira, and M. Colonna.** 2004. Herpes simplex virus type 1 activates murine natural interferon-producing cells through toll-like receptor 9. Blood **103**:1433–1437.
30. **Kumar, H., T. Kawai, H. Kato, S. Sato, K. Takahashi, C. Coban, M. Yamamoto, S. Uematsu, K. J. Ishii, O. Takeuchi, and S. Akira.** 2006. Essential role of IPS-1 in innate immune responses against RNA viruses. J. Exp. Med. **203**:1795–1803.
31. **Luckow, V. A., and M. D. Summers.** 1988. Signals important for high-level expression of foreign genes in Autographa californica nuclear polyhedrosis virus expression vectors. Virology **167**:56–71.
32. **Lund, J., A. Sato, S. Akira, R. Medzhitov, and A. Iwasaki.** 2003. Toll-like receptor 9-mediated recognition of herpes simplex virus-2 by plasmacytoid dendritic cells. J. Exp. Med. **198**:513–520.
33. **Lund, J. M., L. Alexopoulou, A. Sato, M. Karow, N. C. Adams, N. W. Gale, A. Iwasaki, and R. A. Flavell.** 2004. Recognition of single-stranded RNA viruses by Toll-like receptor 7. Proc. Natl. Acad. Sci. USA **101**:5598–5603.
34. **Malmgaard, L., J. Melchjorsen, A. G. Bowie, S. C. Mogensen, and S. R. Paludan.** 2004. Viral activation of macrophages through TLR-dependent and -independent pathways. J. Immunol. **173**:6890–6898.
35. **Matsuura, Y., R. D. Possee, H. A. Overton, and D. H. Bishop.** 1987. Baculovirus expression vectors: the requirements for high level expression of proteins, including glycoproteins. J. Gen. Virol. **68**:1233–1250.
36. **Meylan, E., J. Curran, K. Hofmann, D. Moradpour, M. Binder, R. Bartenschlager, and J. Tschopp.** 2005. Cardif is an adaptor protein in the RIG-I antiviral pathway and is targeted by hepatitis C virus. Nature **437**:1167–1172.
37. **Nallagatla, S. R., J. Hwang, R. Toroney, X. Zheng, C. E. Cameron, and P. C. Bevilacqua.** 2007. 5′-triphosphate-dependent activation of PKR by RNAs with short stem-loops. Science **318**:1455–1458.
38. **Nociari, M., O. Ocheretina, J. W. Schoggins, and E. Falck-Pedersen.** 2007. Sensing infection by adenovirus: Toll-like receptor-independent viral DNA recognition signals activation of the interferon regulatory factor 3 master regulator. J. Virol. **81**:4145–4157.
39. **Pichlmair, A., O. Schulz, C. P. Tan, T. I. Naslund, P. Liljestrom, F. Weber, and C. Reis e Sousa.** 2006. RIG-I-mediated antiviral responses to single-stranded RNA bearing 5′-phosphates. Science **314**:997–1001.
40. **Rasmussen, S. B., L. N. Sorensen, L. Malmgaard, N. Ank, J. D. Baines, Z. J. Chen, and S. R. Paludan.** 2007. Type I interferon production during herpes simplex virus infection is controlled by cell-type-specific viral recognition through Toll-like receptor 9, the mitochondrial antiviral signaling protein pathway, and novel recognition systems. J. Virol. **81**:13315–13324.
41. **Sato, M., H. Suemori, N. Hata, M. Asagiri, K. Ogasawara, K. Nakao, T. Nakaya, M. Katsuki, S. Noguchi, N. Tanaka, and T. Taniguchi.** 2000. Distinct and essential roles of transcription factors IRF-3 and IRF-7 in response to viruses for IFN-alpha/beta gene induction. Immunity **13**:539–548.
42. **Seth, R. B., L. Sun, C. K. Ea, and Z. J. Chen.** 2005. Identification and characterization of MAVS, a mitochondrial antiviral signaling protein that activates NF-kappaB and IRF 3. Cell **122**:669–682.
43. **Stetson, D. B., and R. Medzhitov.** 2006. Recognition of cytosolic DNA activates an IRF3-dependent innate immune response. Immunity **24**:93–103.
44. **Tabeta, K., P. Georgel, E. Janssen, X. Du, K. Hoebe, K. Crozat, S. Mudd, L. Shamel, S. Sovath, J. Goode, L. Alexopoulou, R. A. Flavell, and B. Beutler.** 2004. Toll-like receptors 9 and 3 as essential components of innate immune defense against mouse cytomegalovirus infection. Proc. Natl. Acad. Sci. USA **101**:3516–3521.
45. **Takaoka, A., Z. Wang, M. K. Choi, H. Yanai, H. Negishi, T. Ban, Y. Lu, M. Miyagishi, T. Kodama, K. Honda, Y. Ohba, and T. Taniguchi.** 2007. DAI (DLM-1/ZBP1) is a cytosolic DNA sensor and an activator of innate immune response. Nature **448**:501–505.
46. **Waibler, Z., M. Anzaghe, H. Ludwig, S. Akira, S. Weiss, G. Sutter, and U. Kalinke.** 2007. Modified vaccinia virus Ankara induces Toll-like receptor-independent type I interferon responses. J. Virol. **81**:12102–12110.
47. **Xu, L. G., Y. Y. Wang, K. J. Han, L. Y. Li, Z. Zhai, and H. B. Shu.** 2005. VISA is an adapter protein required for virus-triggered IFN-beta signaling. Mol. Cell **19**:727–740.
48. **Yamamoto, M., S. Sato, H. Hemmi, K. Hoshino, T. Kaisho, H. Sanjo, O. Takeuchi, M. Sugiyama, M. Okabe, K. Takeda, and S. Akira.** 2003. Role of adaptor TRIF in the MyD88-independent toll-like receptor signaling pathway. Science **301**:640–643.
49. **Yoneyama, M., M. Kikuchi, K. Matsumoto, T. Imaizumi, M. Miyagishi, K. Taira, E. Foy, Y. M. Loo, M. Gale, Jr., S. Akira, S. Yonehara, A. Kato, and T. Fujita.** 2005. Shared and unique functions of the DExD/H-box helicases RIG-I, MDA5, and LGP2 in antiviral innate immunity. J. Immunol. **175**:2851–2858.
50. **Yoneyama, M., M. Kikuchi, T. Natsukawa, N. Shinobu, T. Imaizumi, M. Miyagishi, K. Taira, S. Akira, and T. Fujita.** 2004. The RNA helicase RIG-I has an essential function in double-stranded RNA-induced innate antiviral responses. Nat. Immunol. **5**:730–737.
51. **Zheng, M., D. M. Klinman, M. Gierynska, and B. T. Rouse.** 2002. DNA containing CpG motifs induces angiogenesis. Proc. Natl. Acad. Sci. USA **99**:8944–8949.
52. **Zhong, B., Y. Yang, S. Li, Y. Y. Wang, Y. Li, F. Diao, C. Lei, X. He, L. Zhang, P. Tien, and H. B. Shu.** 2008. The adaptor protein MITA links virus-sensing receptors to IRF3 transcription factor activation. Immunity **29**:538–550.
53. **Zhu, J., X. Huang, and Y. Yang.** 2007. Innate immune response to adenoviral vectors is mediated by both Toll-like receptor-dependent and -independent pathways. J. Virol. **81**:3170–3180.

The American Journal of Pathology, Vol. 175, No. 4, October 2009

DOI: 10.2353/ajpath.2009.090102

Immunopathology and Infectious Diseases

Tacrolimus Ameliorates Metabolic Disturbance and Oxidative Stress Caused by Hepatitis C Virus Core Protein

Analysis Using Mouse Model and Cultured Cells

Kyoji Moriya,* Hideyuki Miyoshi,* Takeya Tsutsumi,* Seiko Shinzawa,* Hajime Fujie,* Yoshizumi Shintani,* Hiroshi Yotsuyanagi,* Kohji Moriishi,† Yoshiharu Matsuura,† Tetsuro Suzuki,‡ Tatsuo Miyamura,‡ and Kazuhiko Koike*

From the Department of Internal Medicine, Graduate School of Medicine, University of Tokyo, Tokyo; the Department of Molecular Virology,† Research Institute for Microbial Diseases, Osaka University, Osaka; and the Department of Virology II,‡ National Institute of Infectious Diseases, Tokyo, Japan*

Hepatic steatosis and insulin resistance are factors that aggravate the progression of liver disease caused by hepatitis C virus (HCV) infection. In the pathogenesis of liver disease and metabolic disorders in HCV infection, oxidative stress due to mitochondrial respiratory chain dysfunction plays a pivotal role. Tacrolimus (FK506) is supposed to protect mitochondrial respiratory function. We studied whether tacrolimus affects the development of HCV-associated liver disease using *HCV core gene* transgenic mice, which develop hepatic steatosis, insulin resistance, and hepatocellular carcinoma. Administration of tacrolimus to *HCV core gene* transgenic mice three times per week for 3 months led to a significant reduction in the amounts of lipid in the liver as well as in serum insulin. Tacrolimus treatment also ameliorated oxidative stress and DNA damage in the liver of the *core gene* transgenic mice. Tacrolimus administration reproduced these effects in a dose-dependent manner in HepG2 cells expressing the core protein. The intrahepatic level of tumor necrosis factor-α, which may be a key molecule for the pathogenesis in HCV infection, was significantly decreased in tacrolimus-treated core gene transgenic mice. Tacrolimus thus reversed the effect of the core protein in the pathogenesis of HCV-associated liver disease. These results may provide new therapeutic tools for chronic hepatitis C, in which oxidative stress and abnormalities in lipid and glucose metabolism contribute to liver pathogenesis. *(Am J Pathol 2009, 175:1515–1524; DOI: 10.2353/ajpath.2009.090102)*

Hepatitis C virus (HCV) is a major cause of liver disease; approximately 170 million people are chronically infected worldwide. Persistent HCV infection leads to the development of chronic hepatitis, cirrhosis, and, eventually, hepatocellular carcinoma (HCC), thereby being a serious problem from both medical and socioeconomic viewpoints.[1,2] Recently, a growing amount of evidence showing that HCV infection induces alteration in lipid[3–7] and glucose metabolism has accumulated.[8,9] Augmentation of oxidative stress is also substantiated in HCV infection by a number of clinical and basic studies.[10–13]

We demonstrated previously that the core protein of HCV induces HCC in transgenic mice that have marked hepatic steatosis in the absence of inflammation.[14] In this animal model for HCV-associated HCC, there is augmentation of oxidative stress in the liver during the incubation period.[10] Also noted is an accumulation of lipid droplets that are rich with carbon 18 monounsaturated fatty acids such as oleic and vaccenic acids, which is also observed in liver tissues of patients with chronic hepatitis C com-

Supported in part by a Grant-in-Aid for Scientific Research on Priority Area from the Ministry of Education, Science, Sports and Culture of Japan, by Health Sciences research grants from the Ministry of Health, Labour and Welfare (Research on Hepatitis), and by the Program for Promotion of Fundamental Studies in Health Sciences of the Organization for Drug ADR Relief, R&D Promotion and Product Review of Japan.

Accepted for publication June 22, 2009.

Address reprint requests to Kazuhiko Koike, M.D., Ph.D., Department of Gastroenterology, Internal Medicine, Graduate School of Medicine, University of Tokyo, 7-3-1 Hongo, Bunkyo-ku, Tokyo 113-8655, Japan. E-mail: kkoike-tky@umin.ac.jp.

pared with those in patients with fatty liver due to simple obesity.[15] Recently, we have also shown, using the HCV transgenic mouse model, that the ability of insulin to lower plasma glucose levels is impaired in association with HCV infection,[16] which would be the basis for the frequent development of type 2 diabetes in patients with chronic hepatitis C.[8,9]

Disturbances in lipid and glucose metabolism are notable features of HCV infection and may be profoundly involved in the pathogenesis of liver diseases. Although the mechanism underlying these phenomena is not yet well understood, the development of clues to correct these metabolic disturbances occurring in HCV infection, which have been recently connected to the poor prognosis of patients with chronic hepatitis C, is awaited. Moreover, a key role for oxidative stress in the pathogenesis of hepatitis C,[11,12] which may be closely associated with the aforementioned metabolic disorders, has been identified. The association of oxidative stress augmentation in HCV infection with mitochondrial respiratory dysfunction[10,13,17] suggests that one possibility to ameliorate such a condition is the use of agents that can protect the mitochondrial respiratory function.

We have conducted information retrieval and screening for agents that can protect the mitochondrial respiratory function. Tacrolimus (FK506), which is widely used in organ transplantation, is one such agent with evidence showing protection of the mitochondrial respiratory function,[18–21] although it shows no antiviral effect. We explored, using transgenic mouse and cultured cell models that express the HCV core protein, whether tacrolimus improves metabolic disturbances including lipid and glucose homeostases as well as oxidative stress augmentation through a possible involvement of mitochondrial function.

Materials and Methods

Transgenic Mouse and Cultured Cells

The production of *HCV core gene* transgenic mice has been described previously.[6] Mice were cared for according to institutional guidelines with the approval by the institutional review board of the animal care committee, fed an ordinary chow diet (Oriental Yeast Co., Ltd., Tokyo, Japan), and maintained in a specific pathogen-free state. Because there is a sex preference in the development of liver lesions in the transgenic mice, we used only male mice. At least five mice were used in each experiment, and the data were subjected to statistical analysis. HepG2 cell lines expressing the HCV core protein under the control of the CAG promoter (Hep39J, Hep396, and Hep397) or a control HepG2 line (Hepswx) carrying the empty vector were described previously.[22,23] Bulk HepG2 cells were also used as a control.

Reagents

Cholesterol esters and lipid standards were purchased from Sigma-Aldrich (St. Louis, MO), and glycogen and amyloglucosidase were obtained from Seikagaku Kogyo (Tokyo, Japan). Other chemicals were of analytical grade and were purchased from Wako Chemicals (Tokyo, Japan). Tacrolimus (FK506) was kindly provided by Astellas Pharma Inc. (Tokyo, Japan). Cyclosporine A (CyA) was purchased from Sigma-Aldrich.

Administration of Tacrolimus and Cyclosporine A

Tacrolimus (0.1 mg/kg b.wt., suspended in mannitol and hydroxychlorinated caster oil [HCO-60]), or vehicle only was administered to the core gene transgenic or control mice i.p., three times per week for 3 months beginning at 3 months of age. For *in vitro* experiments, tacrolimus was added to the culture medium at the final concentration of 0 nmol/L, 10 nmol/L, 100 nmol/L, or 1 μmol/L. CyA was also added to the culture medium at the same concentrations.

Assessment of Glucose Homeostasis

Blood was drawn at different time points from the tail vein, and plasma glucose concentrations were measured using an automatic biochemical analyzer (DRI-CHEM 3000V, Fuji Film, Tokyo, Japan). The levels of serum insulin were determined by radioimmunoassay (Biotrak, Amersham Pharmacia Biotech, Piscataway, NJ) using rat insulin as a standard. For the determination of the fasting plasma glucose level, the mice were fasted for >16 hours before the study. An insulin tolerance test was performed as described previously.[16]

Lipid Extraction, Measurement of Triglyceride Content, and Analysis of Fatty Acid Compositions

Lipid extraction from the mouse liver tissues or cultured cells was performed as described previously.[15,24] For the analysis of fatty acid compositions, the residue was methanolysed by the modified Morrison and Smith method with boron trifluoride as a catalyst.[25] Fatty acid methyl esters were analyzed using a Shimadzu GC-7A gas chromatograph (Shimadzu Corp., Kyoto, Japan) equipped with a 30-m-long × 0.3-mm diameter support coated with ethylene glycol succinate.[24]

Evaluation of Oxidative and Antioxidative System

Lipid peroxidation was estimated spectrophotometrically using thiobarbituric acid-reactive substances and is expressed in terms of malondialdehyde formed per milligram protein. Reduced glutathione and oxidized glutathione levels were measured as described previously.[10] The total amount of glutathione was calculated by adding the amounts obtained for glutathione and oxidized glutathione. For the evaluation of DNA damage in cells, apurinic/apyrimidinic sites were determined using a DNA Damage Quantification Kit (Dojindo Molecular Technolo-

gies, Inc., Tokyo, Japan) following the manufacturer's protocol.

Determination of Reactive Oxygen Species

Cells were plated onto glass coverslips and examined for reactive oxygen species (ROS) production as a marker for oxidative stress. They were loaded for 2 hours with chloromethyl 2′,7′-dichlorodihydrofluorescein diacetate (Molecular Probes Inc., Eugene, OR) at a final concentration of 10 μmol/L.[26] Results were expressed as relative fluorescence intensity and normalized to the control cells. In some experiments, ROS was measured after the incubation with tacrolimus or CyA.

Measurement of Ketone Body Ratio

For the determination of ketone body ratio (KBR), cells were cultured to confluence on a 3.5-cm dish, and the medium was replaced with 700 μl of fresh medium. For arterial KBR, the mice were fasted for >16 hours, followed by the drawing of arterial blood. After a 24-hour incubation, acetoacetate and β-hydroxybutyrate in the medium were measured by monitoring the production or consumption of NADH with a Ketorex kit (Sanwa Chemical, Nagoya, Japan).[27] The KBR was calculated as the acetoacetate/β-hydroxybutyrate ratio.

Microarray Analysis

An Affymetrix GeneChip analysis cDNA array system (Mouse Genome 430A 2.0, Kurabo, Osaka, Japan) was used for the analysis. Two thousand species of mouse DNA fragments were spotted on the filter. Genes that were 1.5-fold increased or decreased in both of the two tacrolimus-treated mice compared with mice treated with vehicle were defined as up-regulated or down-regulated, respectively.

Real-Time PCR and Western Blotting

RNA was prepared from mouse liver tissues using TRIzol LS (Invitrogen, Carlsbad, CA). The first-strand cDNAs were synthesized with a first-strand cDNA synthesis kit (Amersham Pharmacia Biotech, Franklin Lakes, NJ). The fluorescent signal was measured with an ABI Prism 7000 system (Applied Biosystems, Tokyo, Japan).

The genes encoding mouse *tumor necrosis factor (TNF)-α, sterol regulatory element binding protein (SREBP)-1c, resistin, stearoyl-CoA desaturase (SCD)-1, and hypoxanthine phosphoribosyltransferase* were amplified with the primer pairs 5′-GACAAGGTGGGCTACGGGCTTG-3′ and 5′-TCCCAAATGGGCTCCCTCT-3′, 5′-ACGGAGCCATGGATTGCACATTTG-3′ and 5′-TACATCTTTAAAGCAGCGGGTGCCGATGGT-3′, 5′-GAAGGCACAGCAGTCTTGA-3′ and 5′-GCGACCTGCAGCTTACAG-3′, 5′-TTCCCTCCTGCAAGCTCTAC-3′ and 5′-CGCAAGAAGGTGCTAACGAAC-3′, and 5′-CCAGCAAGCTTGCAACCTTAACCA-3′ and 5′-GTAATGATCAGTCAACGGGGGAC-3′, respectively. The sense and antisense primers were located in different exons to avoid false-positive amplification from contaminated genomic DNA. Each PCR product was confirmed as a single band of the correct size by agarose gel electrophoresis (data not shown).

Reporter Assay for SREBP-1c Promoter Activity

A plasmid encoding firefly luciferase under the control of the *SREBP-1c* promoter (pGL3-srebp-1cPro) and a control plasmid encoding *Renilla* luciferase (Promega, Madison, WI) were transfected into 293T cells. Tacrolimus was added at a final concentration of 100 nmol/L to the culture medium of 293T cells transfected with pGL3-srebp-1cPro with or without an expression plasmid of HCV core protein at 24 hours after transfection. Cells were harvested 24 hours after treatment. Luciferase activity was measured by using the dual-luciferase reporter assay system (Promega). Firefly luciferase activity was standardized with that of *Renilla* luciferase, and the results are expressed as the fold-increase in relative luciferase units.

Statistical Analysis

Data are presented as the mean ± SE. The significance of the difference in means was determined by a Mann-Whitney *U* test wherever appropriate. $P < 0.05$ was considered significant.

Results

Effect of Tacrolimus on Insulin Resistance Induced by HCV

The *core gene* transgenic mice exhibit insulin resistance in the absence of obesity from the age of 2 months.[16] In tacrolimus-treated mice, there was a slight, but not significant, reduction in body weight compared with control mice at the end of tacrolimus administration at 6 months of age (Figure 1A). Tacrolimus administration to the *core gene* transgenic mice restored the plasma glucose levels to within normal limit (Figure 1B) ($P < 0.05$), whereas it caused no significant reduction in the control mice. The plasma glucose levels in the vehicle-treated core gene transgenic mice were higher than those in the core gene transgenic mice reported previously,[16] probably owing to the older age of mice in the current study than in the previous one. The levels of serum insulin were also significantly reduced by the treatment with tacrolimus for 3 months in the core gene transgenic mice, whereas there was no significant change in the control mice (Figure 1C). The reduction in both plasma glucose and serum insulin levels indicates that the administration of tacrolimus restored the resistance to insulin action, which is attributed to the suppression of insulin action in the liver by the core protein.[16] Actually, an insulin tolerance test (1 U/kg b.wt.) demonstrated the improvement of insulin action in the tacrolimus-treated core gene transgenic mice (Figure 1D).

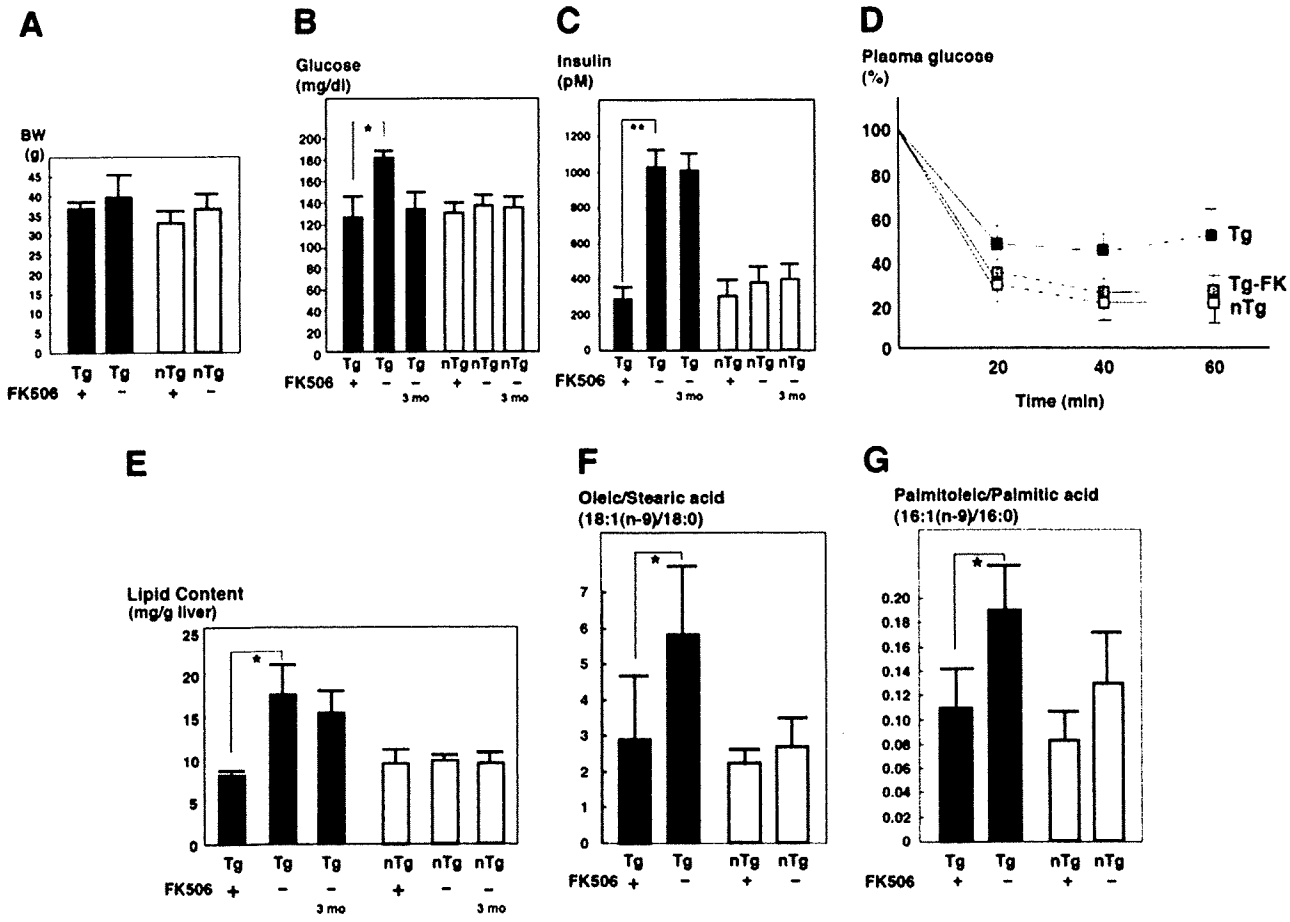

Figure 1. Effect of tacrolimus (FK506) on glucose and lipid metabolism in the core gene transgenic mice. Tacrolimus (0.1 mg/kg b.wt.) or vehicle was administered to core gene transgenic or control mice i.p., three times weekly for 3 months beginning at 3 months of age. **A:** Body weight at the baseline and end of treatment. **B:** Plasma glucose level. **C:** Serum insulin level. **D:** Insulin tolerance test. Black boxes represent core gene transgenic mice; white boxes represent control mice; gray boxes represent core gene transgenic mice treated with tacrolimus (Tg-FK). **E:** Total lipid content in the liver. **F:** Ratio of oleic/stearic acid [18:1(n-9)/18:0]. **G:** Ratio of palmitoleic/palmitic acid [16:1(n-9)/16:0]. black bars represent transgenic mice; white bars represent control mice. Tg 3 mo indicates 3-month-old transgenic mice showing the baseline state just before FK treatment, and Tg indicates 6-month-old transgenic mice, either with or without tacrolimus treatment for 3 months. Values represent the mean ± SE, $n = 5$ in each group. $^{*}P < 0.05$. Tg, transgenic mice; nTg, nontransgenic control mice. $^{**}P < 0.01$.

Tacrolimus Improves Lipid Metabolism Disorders in Mice

We then studied whether tacrolimus administration affects lipid metabolism in the mice. The core gene transgenic mice developed a marked hepatic steatosis.[6,14] In addition, the composition of accumulated lipid was different from that in the fatty liver as a result of simple overnutrition: carbon 18 or 16 monounsaturated fatty acid levels were significantly increased.[15] As shown in Figure 1E, the tacrolimus treatment significantly reduced the lipid content in liver tissues compared with the vehicle treatment of the core gene transgenic mice ($P < 0.05$, $n = 5$ each), whereas there was no change in the control mice. The increased ratios of oleic to stearic acid [18:1 (n-9)/18:0] and palmitoleic to palmitic acid [16:1(n-9)/16:0] in the core gene transgenic mice returned to levels similar to those in control mice (Figure 1, F and G) ($P < 0.05$). Thus, the administration of tacrolimus for 3 months restored the abnormalities in lipid metabolism that were induced by the core protein of HCV. Histologically, tacrolimus significantly improved steatosis in the liver of core gene transgenic mice, in which micro- and macrovesicular lipid droplets were accumulated in hepatocytes, chiefly around the central veins of the liver (Figure 2A). There was no sign of inflammation in the liver with or without the tacrolimus treatment.

Effect of Tacrolimus on Lipid Metabolism in HepG2 Cells Expressing HCV Core Protein

To further prove the ameliorating effect of tacrolimus on lipid metabolism, we then performed experiments using HepG2 cells that express the core protein.[22,23] HepG2 cells, the lipid metabolism of which is somewhat different from that in normal hepatocytes,[28] show a significant increase in the level of 5,8,11-eicosatrienoic acid [20:3 (n-9)], as a result of activations of the fatty acid enzymes, Δ^9-, Δ^6-, and Δ^5-desaturases, by the core protein (H. Miyoshi and K. Koike, unpublished data). Incubation of the core-expressing HepG2 cells with tacrolimus at 100 nmol/L and 1 μmol/L for 48 hours significantly reduced the accumulation of 20:3(n-9), whereas CyA treat-

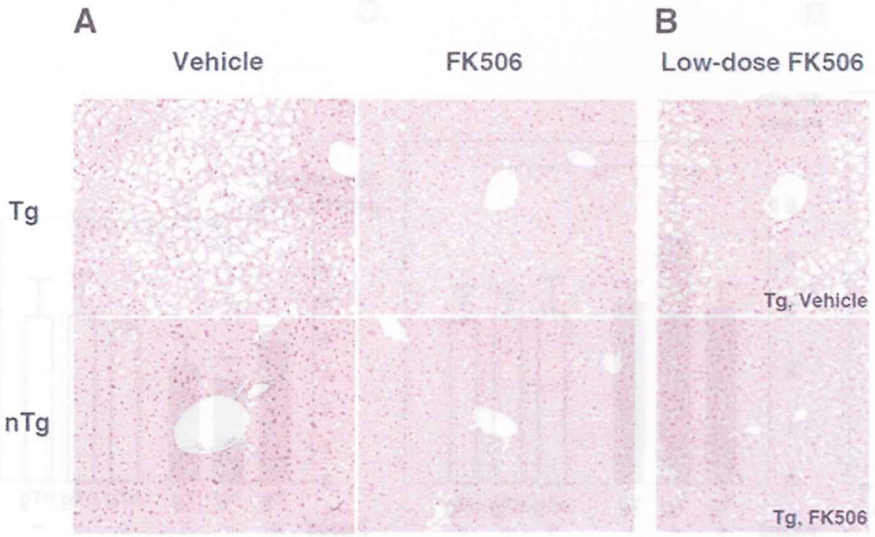

Figure 2. Morphological analysis of the liver of the core gene transgenic mice. Representative cases are shown either treated with tacrolimus (FK506) or vehicle (H&E staining). **A:** There is a prominent improvement of steatosis in the 3-month tacrolimus-treated core gene transgenic mice compared with the vehicle-treated mice. **B:** A prominent improvement in steatosis was also obtained by the administration of one-fifth dose of tacrolimus for 1 month beginning at 3 months of age. For histological analysis, two independent researchers evaluated 40 microscopic fields each, and a representative picture is shown for each category. Original magnification, ×125. Tg, transgenic mice; nTg, nontransgenic control mice.

ment increased the level of 20:3(n-9) in a dose-dependent manner in the core-expressing HepG2 cells (Figure 3, A and B). Neither tacrolimus nor CyA changed the 20:3(n-9) content in HepG2 cells that do not express the core protein.

Low Dose of Tacrolimus Also Ameliorates Steatosis and Insulin Resistance

Because the usual dose of tacrolimus for liver transplantation naturally induces an immunosuppressed state in patients, we conducted a mouse study with a tacrolimus dose lower than that in the aforementioned study. In this low-dose experiment, tacrolimus at 0.02 mg/kg b.wt. (one-fifth of the previous one) was administered to mice for 1 month from the age of 3 months. Similar to the results with the dose of 0.1 mg/kg b.wt., there were significant decreases in the lipid content in the liver (9.5 ± 0.8 [0.02 mg/kg b.wt. tacrolimus] versus 18.7 ± 4.4 [vehicle only] mg/g liver; $P < 0.05$) and serum insulin concentration (96.6 ± 16.9 [0.02 mg/kg b.wt. tacrolimus] versus 1137.1 ± 88.0 [vehicle only] pmol/L; $P < 0.05$) in the core gene transgenic mice treated with tacrolimus. Histological changes are shown in Figure 2B.

Effect of Tacrolimus on Oxidative Stress and Antioxidative System in Mice

We next examined whether the 3-month administration of tacrolimus affects the redox state in the core gene transgenic mice. In the liver of the core gene transgenic mice, the ROS level was higher than that in the liver of control mice as determined by lipid peroxidation.[10] Treatment with tacrolimus significantly reduced the level of thiobarbituric acid-reactive substances in the liver of the core gene transgenic mice (Figure 4A) ($P < 0.05$). As a result of oxidative stress overproduction, there was damage in the DNA of hepatocytes of the core gene transgenic mice from a young age.[10] To evaluate the effect of tacrolimus on the nuclear DNA damage, the apurinic/apyrimidinic site index was determined in liver tissues from the core gene transgenic mice. As shown in Figure 4B, the apurinic/apyrimidinic site index in the liver of the core gene transgenic mice, which was significantly higher

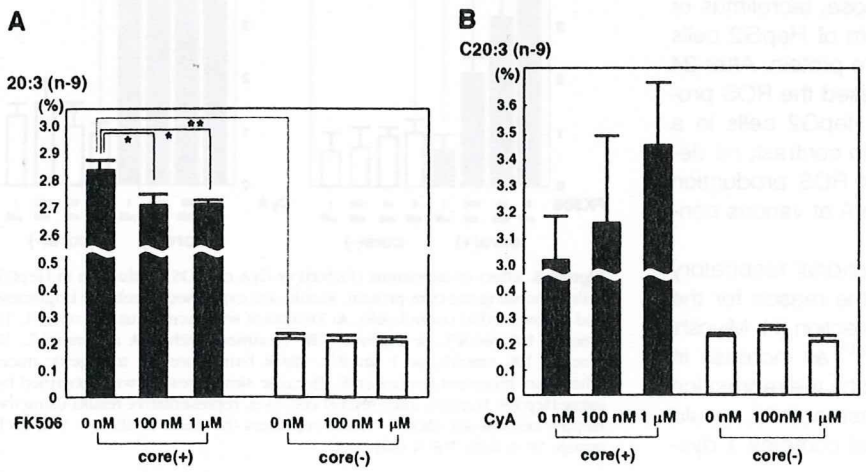

Figure 3. Effect of tacrolimus (FK506) or CyA on fatty acid compositions in HepG2 cells expressing the core protein. The fatty acid compositions of the total cell lipids were analyzed, and the percentage of 5,8,11-eicosatrienoic acid [20:3(n-9)] in the core-expressing and control HepG2 cells was calculated. **A:** Treatment with tacrolimus at 0 nmol/L, 100 nmol/L, or 1 μmol/L. **B:** Treatment with CyA at 0 nmol/L, 100 nmol/L, or 1 μmol/L. Black bars represent core-expressing cells; white bars represent control cells. Because similar results were obtained by using Hep39J, Hep396, and Hep397 cell lines, representative results using the Hep39J cell line are shown. Values represent the mean ± SE; $n = 5$ in each group. $^{*}P < 0.05$ and $^{**}P < 0.01$.

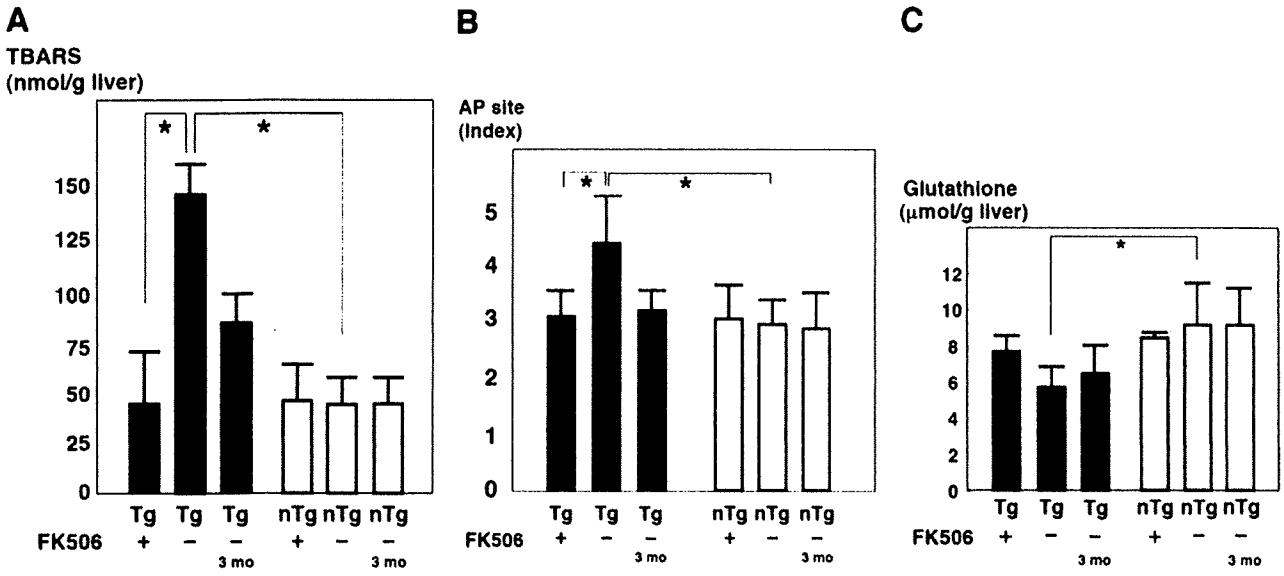

Figure 4. Effect of tacrolimus (FK506) on oxidative stress in the core gene transgenic mice. Tacrolimus (0.1 mg/kg b.wt.) or vehicle only was administered to the core gene transgenic or control mice for 3 months. **A:** Lipid peroxidation in the liver. **B:** apurinic/apyrimidinic (AP) site in the liver as a marker of nuclear DNA damage; **C:** Total glutathione level in the liver. Black bars represent transgenic mice; white bars represent control mice. Tg 3 mo indicates 3-month-old transgenic mice, showing the baseline state just before tacrolimus treatment, and Tg indicates 6-month-old transgenic mice, either with or without 3 months of tacrolimus treatment. Values represent the mean ± SE; $n = 5$ in each group. $^*P < 0.05$. Tg, transgenic mice; nTg, nontransgenic control mice. TBARS, thiobarbituric acid-reactive substances.

than that in the control mice, was significantly decreased by the tacrolimus treatment to a level similar to that in the control mice ($P < 0.05$).

The level of glutathione, one of the antioxidant systems, was significantly decreased in the liver of the core gene transgenic mice presumably as a result of oxidative stress overproduction but returned to a level similar to that in the control mice after the 3-month administration of tacrolimus, although the difference was not statistically significant ($P = 0.063$) (Figure 4C). Thus, the oxidative stress augmentation induced by the core protein of HCV was reduced by tacrolimus.

Effect of Tacrolimus on Oxidative Stress in Core-Expressing HepG2 Cells

Evidence for scavenging ROS by the administration of tacrolimus to the mice prompted us to validate this finding using cultured cells. For this purpose, tacrolimus or CyA was added to the culture medium of HepG2 cells that express or do not express the core protein. After 24 hours of incubation, tacrolimus decreased the ROS production level in the core-expressing HepG2 cells in a dose-dependent manner (Figure 5A). In contrast, no decrease but rather an augmentation of ROS production was observed by the treatment with CyA at various concentrations (Figure 5B).

Because dysfunction of the mitochondrial respiratory chain complex 1 is suspected to be the reason for the ROS production associated with HCV infection (H. Miyoshi and K. Koike, unpublished data),[12,13,17] an increase in the NADH/NAD$^+$ ratio, which is caused by the repression of the complex 1 NADH dehydrogenase activity, would be a good marker for the mitochondrial complex 1 dysfunction. Therefore, we evaluated the effect of tacrolimus on the accumulation of NADH in the core-expressing HepG2 cells. The NADH/NAD$^+$ ratio, which is strictly estimated from a reciprocal of KBR,[26,29] was significantly higher in the core gene transgenic mice than in control mice (1/atrial KBR) and in HepG2 cells expressing the core protein than in control cells (1/KBR) (Figure 6A). By the treatment with 1 μmol/L tacrolimus, the ratio significantly decreased compared with the baseline (Figure 6B), whereas CyA treatment caused no effect in the core-expressing HepG2 cells (Figure 6C), as was the

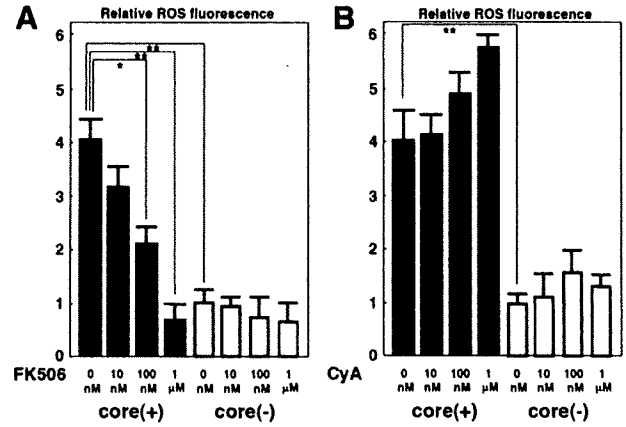

Figure 5. Effect of tacrolimus (FK506) or CyA on ROS production in HepG2 cells expressing the core protein. Results are expressed as relative brightness and normalized to control cells. **A:** Treatment with tacrolimus at 0 nmol/L, 10 nmol/L, 100 nmol/L, or 1 μmol/L. **B:** Treatment with CyA at 0 nmol/L, 10 nmol/L, 100 nmol/L, or 1 μmol/L. Black bars represent transgenic mice; white bars represent control cells. Because similar results were obtained by using Hep39J, Hep396, and Hep397 cell lines, representative results using the Hep39J cell line are shown. Values represent the mean ± SE; $n = 5$ in each group. $^*P < 0.05$; $^{**}P < 0.01$.

case in the determination of ROS by chloromethyl 2′,7′-dichlorodihydrofluorescein diacetate.

Changes in Gene Expression by Tacrolimus Treatment of Mice

We then performed a comprehensive microarray analysis of gene expression in the liver, which was up- or down-regulated by tacrolimus. For this analysis, the tacrolimus-treated mice were compared with the vehicle-treated mice, in two pairs of the core gene transgenic and control mice, respectively. Genes that were 1.5-fold increased or decreased in both of the two tacrolimus-treated mice compared with those treated with vehicle were defined as up-regulated or down-regulated, respectively. As shown in Table 1, several genes were found to be up-regulated or down-regulated in both the core gene transgenic and control mice after the treatment with tacrolimus for 3 months. A number of genes including that for TNF-α were up- or down-regulated both in the core gene transgenic and control mice. In contrast, the expressions of some genes including that for resistin were differentially regulated between the core gene transgenic and control mice. The expressions of these genes were confirmed by real-time PCR analysis.

Then, to explore the mechanism by which tacrolimus reverses the pathological effect of the core protein in the liver, we examined, by real-time PCR analysis, the expression of some cellular genes including TNF-α, SREBP-1c, SCD-1, and proteasome activator 28-γ. These genes or gene products have been suggested to play a pivotal role in the pathogenesis of HCV-associated liver disease.[30,31] TNF-α and SREBP-1c genes have been shown to be up-regulated in the liver of the core gene transgenic mice and considered to play a role in the development of insulin resistance and steatosis.[30,31] By the treatment of the core gene transgenic mice with tacrolimus for 3 months, there was a significant decrease in the mRNA level of both TNF-α and SREBP-1c (Figure 7, A–C) ($P < 0.05$). The SCD-1 mRNA level was also reduced in the tacrolimus-treated core gene transgenic mice. Because down-regulation of SREBP-1c expression by tacrolimus was observed only in the core gene transgenic mice but not in control mice, it is estimated that tacrolimus antagonizes the action of core protein in its transactivating function of the SREBP-1c promoter. The down-regulation of SREBP-1c, then, would lead to the suppression of SCD-1 expression and amelioration of steatosis. We confirmed this by conducting luciferase assays using cultured cells. As shown in Figure 7D, tacrolimus cancelled the effect of the core protein on the activation of SREBP-1c gene promoter. The level of the proteasome activator 28-γ protein, which is indispensable for the action of the core protein in the pathogenesis of HCV-associated liver lesion,[31] was determined by Western blotting, but there was no change caused by the tacrolimus treatment (data not shown).

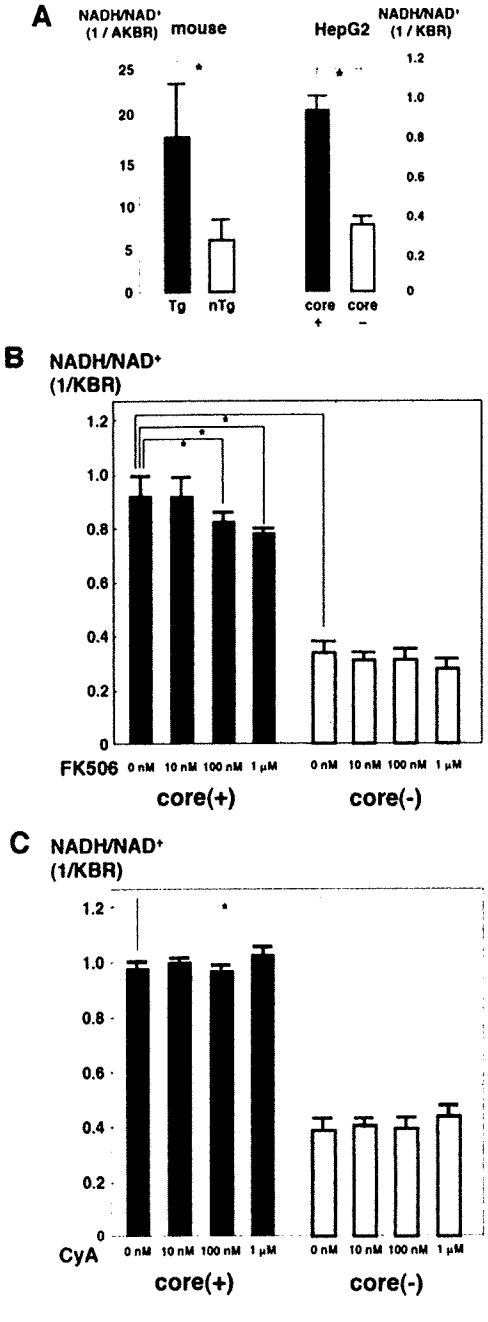

Figure 6. Effect of tacrolimus (FK506) or CyA on NADH accumulation in HepG2 cells expressing the core protein. **A:** NADH/NAD$^+$ was determined in mice (left) or HepG2 cells (right) with or without the core protein. **B:** The ketone body ratio was determined in HepG2 cells with or without the core protein after incubation with tacrolimus for 24 hours at 0 nmol/L, 10 nmol/L, 100 nmol/L, or 1 μmol/L. **C:** The ketone body ratio was determined in HepG2 cells with or without the core protein after incubation with CyA for 24 hours at 0 nmol/L, 10 nmol/L, 100 nmol/L, or 1 μmol/L. Black bars represent transgenic mice; white bars represent control cells. Because similar results were obtained by using Hep39J, Hep396 and Hep397 cell lines, representative results using the Hep39J cell line are shown. Values represent the mean ± SE; $n = 5$ in each group. *$P < 0.05$. AKBR, arterial KBR; Tg, transgenic mice; nTg, nontransgenic mice.

Discussion

Antiviral treatment for chronic hepatitis C has advanced markedly. Nearly 50% of patients with chronic hepatitis C

Table 1. Genes Whose Expression Levels in the Mouse Liver Were Altered by the Treatment with FK506

	Up-regulated in Tg	Down-regulated in Tg
Up-regulated in nTg	Nuclear factor, erythroid derived 2	Resistin
	DNA segment, human D6S2654E	Resistin like alpha
	Fatty acid binding protein 5	Nuclear receptor subfamily 4, group A, member
	epidermal squalene epoxidase	insulin-like growth factor binding protein 1
	Zinc finger protein 69	calcium and integrin binding family member 3
Down-regulated in nTg	X-linked lymphocyte-regulated 4	Tumor necrosis factor alpha
	Cytochrome P450, family 2,	Cytochrome P450, family 17, subfamily a,
	subfamily b, polypeptide 9	polypeptide 1
	X-linked lymphocyte-regulated 3a	B-cell leukemia/lymphoma 6
	Signal sequence receptor, delta	

Genes with altered expression in Tg (columns) or in nTg (rows) are described in a 4 × 4 table. Genes that were 1.5-fold increased or decreased in both of the two FK506-treated mice compared with those treated with placebo were defined as up-regulated or down-regulated, respectively. Tg, core gene transgenic mouse; nTg, nontransgenic control mouse.

with HCV genotype 1 and high viral loads achieve a sustained virological response as a result of ribavirin/peginterferon combination therapy.[32,33] However, the remaining patients who could not achieve sustained virological response continue to experience progression of chronic hepatitis and have a high probability for development of HCC. Although therapies with new agents such as viral protease or RNA polymerase inhibitors are being developed, there is hope for development of the means to retard the progression of chronic hepatitis.

Recently, evidence showing that hepatic steatosis and insulin resistance are crucial determinants of the progression of liver fibrosis has accumulated.[34–37] Moreover, the importance of oxidative stress, which is closely associated with metabolic disorders such as insulin resistance and steatosis, is implicated in the pathogenesis of HCV-associated liver disease. Given the suggested association of oxidative stress augmentation with the dysfunction of mitochondrial respiration in HCV infection,[12,13,17] one possibility to ameliorate such a condition is the use of agents that can protect the mitochondrial respiratory function. Tacrolimus is one such agent with evidence of providing protection of the mitochondrial respiratory function,[18–21] although it does not show an antiviral effect.

In the current study, the administration of tacrolimus significantly improved the disturbances in lipid and glucose metabolism both *in vivo* and *in vitro*. As disorders of lipid metabolism associated with HCV infection, hepatic steatosis and increases in monounsaturated fatty acid levels have been demonstrated.[3,4,6,7,15] The latter is caused by the activation of fatty acid enzymes such as Δ^9- or Δ^6-desaturase, resulting in increases in 18:1(n-9)/18:0 and 16:1(n-9)/16:0 ratios (H. Miyoshi and K. Koike, unpublished data).[15] Tacrolimus ameliorated these lipid alterations associated with HCV infection with no impact on mouse body weight. Tacrolimus also improved the insulin resistance in the HCV mouse model, in which tyrosine phosphorylation of insulin receptor substrate-1 is impaired by the HCV core protein.[16]

Moreover, tacrolimus treatment ameliorated oxidative stress augmentation, which is considered to play a pivotal role in the progression of liver disease or the development of HCC in HCV infection.[10–13] In mice transgenic for the HCV core gene, in which DNA damage develops because of oxidative stress augmentation,[13] tacrolimus decreased the levels of peroxylipid and DNA damage formations. Dysfunction of the mitochondrial respiratory chain complex 1 is suspected to be a source of ROS overproduction in HCV infection.[12,13,17] To assess changes in mitochondrial complex 1 function caused by tacrolimus, the NADH/NAD^+ ratio, which reflects the complex 1 NADH dehydrogenase activity, was determined in HepG2 cells expressing the core protein. The NADH/NAD^+ ratio, which is strictly estimated from a reciprocal of KBR (1/atrial KBR),[26,29] was significantly re-

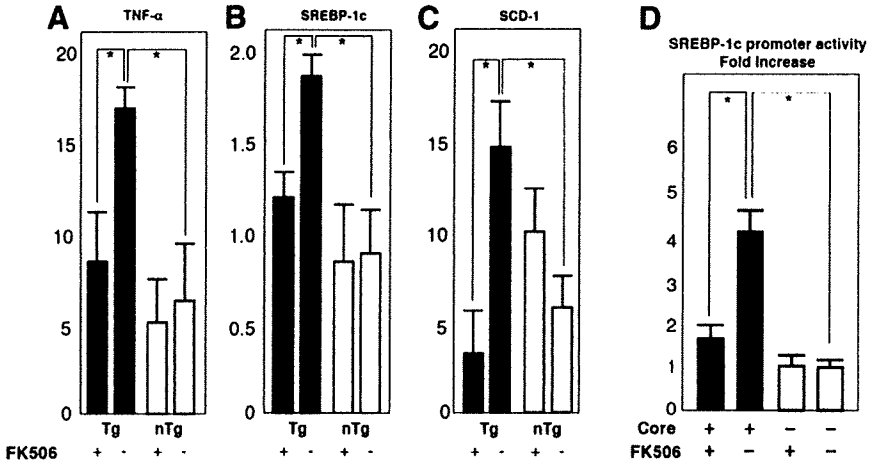

Figure 7. A–C: Effect of tacrolimus (FK506) on mRNA levels of cellular genes. The mRNA levels of TNF-α (**A**), SREBP-1c (**B**), and SCD-1 (**C**) genes were determined by real-time PCR analysis in the tacrolimus- or vehicle-treated mouse livers. The transcriptions of the genes were normalized with that of hypoxanthine phosphoribosyltransferase, and the values are expressed as relative activities. **D:** Effect of tacrolimus on the transactivating function of the core protein on the SREBP-1c promoter. A luciferase assay was performed using a plasmid encoding firefly luciferase under the control of the SREBP-1c promoter with or without the expression of HCV core protein. Tacrolimus was added at a final concentration of 100 nmol/L to the culture medium. Black bars represent transgenic mice; white bars represent control cells. Values represent the mean ± SE; $n = 5$ in each group. $^*P < 0.05$. Tg, transgenic mice; nTg, nontransgenic mice.

duced by the addition of tacrolimus but not CyA. Thus, tacrolimus protected the mitochondrial respiratory chain complex 1 function from the impact of the core protein, decreased oxidative stress, and improved steatosis and insulin resistance.

Some of features induced by the core protein including steatosis, insulin, and DNA damage were already present in the core gene transgenic mice at 3 months of age as the baseline, and those were improved by tacrolimus treatment. This fact indicates that tacrolimus is not only preventing the development of core-induced features but also reversing such changes in the mouse liver.

The tacrolimus dose used in the current study was 0.1 mg/kg b.wt. This is the same dose as that used in recipients of liver or kidney transplantation. The result of a subexperiment with a lower tacrolimus dose of 0.02 mg/kg b.wt. was similar to that with the dose of 0.1 mg/kg b.wt. This finding is promising because it indicates that the "anti-core protein effect" may be achievable at such a low dose of tacrolimus without provoking strong immunosuppression. The tacrolimus concentration (100 nmol/L) that caused the anti-core protein effect in the cultured cell study is similar to that in the blood of recipients of liver transplantation and much lower than those used in previous studies.[19,38] In the current study, tacrolimus was administered only i.p., although it tacrolimus is administered i.v. or p.o. in humans. Therefore, a concern may arise regarding the administration route. Because the bioavailability of tacrolimus is approximately 25% (range from 5 to 93%) in human patients,[39] a difference in the concentrations of tacrolimus may be possible between i.p. and p.o. administration. However, in human patients, target levels of tacrolimus concentration are generally achieved by p.o. administration as the maintenance therapy. Therefore, the target concentration would be achieved in mouse models by p.o. administration for 3 months as it is in human patients. Our current results strongly support the notion that tacrolimus can protect the mitochondrial respiratory function, resulting in a reduction of ROS production.

There is also a controversy concerning the effect of tacrolimus on glucose homeostasis. Post-transplantation diabetes is a complication in kidney or liver transplantation.[40,41] *In vivo* and *in vitro* studies have shown that tacrolimus may inhibit insulin secretion from the pancreatic β-cells.[40] Thus, tacrolimus may have a potential to induce diabetes. However, there have been no well designed studies on this specific point: in one study, corticosteroid withdrawal from tacrolimus-based immunosuppression reduced insulin resistance without changing insulin secretion.[41] In our study using the HCV mouse model, tacrolimus administration at the dose similar to those in organ transplant recipients decreased serum insulin levels without increasing plasma glucose levels. These results point toward the future use of tacrolimus *in vivo* for the amendment of metabolic abnormalities, such as steatosis and insulin resistance, associated with HCV infection. However, it should be noted that there is a difference between our mouse model and human patients. Organ transplant recipients generally have injury to other bodily organs after a prolonged course of illness, whereas the mouse model we have exploited does not. In addition, our mouse model originally has insulin resistance with the presence of hyperplasia of Langerhans islands.[16] Therefore, the effect of tacrolimus on glucose homeostasis in the current mouse study may not be exactly applicable to human patients.

The results of the gene expression analysis by microarray and subsequent real-time PCR were of considerable interest. Tacrolimus reduced the mRNA levels of TNF-α, SCD-1, and SREBP-1c genes, which are elevated in both patients with chronic hepatitis C and HCV core gene transgenic mice.[30,31] The elevation in the TNF-α level causes insulin resistance *in vivo*, which is also observed in HCV core gene transgenic mice.[16] The elevations in SREBP-1c and SCD-1 gene mRNA levels cause the overproduction of triglycerides, leading to the development of steatosis. The reductions in the expression levels of these genes may explain the effect of tacrolimus on the improvement of steatosis, insulin resistance, and oxidative stress in these HCV models. Although recent investigations have shown that the immunosuppressive drugs tacrolimus and rapamycin inhibit the expression of different inflammatory mediators,[42,43] the anti-inflammatory functions of these drugs are not well established. Our *in vitro* and *in vivo* experiments confirmed that tacrolimus inhibited the induction of ROS generation, which is mediated by the core protein. Our data indicate that the inhibition of ROS formation may explain part of the favorable effect of immunosuppressive agents on inflammatory conditions.

In conclusion, our results demonstrate that tacrolimus has protective potential against damage caused by the HCV core protein including the induction of steatosis, insulin resistance, and oxidative stress, both in mice and cultured cells. Although more studies are required to elucidate the precise mechanism underlying the potential of tacrolimus in reversing the pathogenesis in HCV infection, these results may provide new therapeutic tools for chronic hepatitis C, in which oxidative stress and abnormalities in lipid and glucose metabolism contribute to liver pathogenesis.

References

1. Saito I, Miyamura T, Ohbayashi A, Harada H, Katayama T, Kikuchi S, Watanabe Y, Koi S, Onji M, Ohta Y, Choo Q, Houghton M, Kuo G: Hepatitis C virus infection is associated with the development of hepatocellular carcinoma. Proc Natl Acad Sci USA 1990, 87:6547–6549
2. Simonetti RG, Camma C, Fiorello F, Cottone M, Rapicetta M, Marino L, Fiorentino G, Craxi A, Ciccaglione A, Giuseppetti R, Stroffolini T, Pagliaro L: Hepatitis C virus infection as a risk factor for hepatocellular carcinoma in patients with cirrhosis. Ann Intern Med 1992, 116:97–102
3. Scheuer PJ, Ashrafzadeh P, Sherlock S, Brown D, Dusheiko GM: The pathology of chronic hepatitis C. Hepatology 1992, 15:567–571
4. Bach N, Thung SN, Schaffner F: The histological features of chronic hepatitis C and autoimmune chronic hepatitis: a comparative analysis. Hepatology 1992, 15:572–577
5. Barba G, Harper F, Harada T, Kohara M, Goulinet S, Matsuura Y, Eder G, Schaff Z, Chapman MJ, Miyamura T, Bréchot C: Hepatitis C virus core protein shows a cytoplasmic localization and associates to cellular lipid storage droplets. Proc Natl Acad Sci USA 1997, 94:1200–1205
6. Moriya K, Yotsuyanagi H, Shintani Y, Fujie H, Ishibashi K, Matsuura Y, Miyamura T, Koike K: Hepatitis C virus core protein induces hepatic steatosis in transgenic mice. J Gen Virol 1997, 78:1527–1531

7. Lerat H, Honda M, Beard MR, Loesch K, Sun J, Yang Y, Okuda M, Gosert R, Xiao SY, Weinman SA, Lemon SM: Steatosis and liver cancer in transgenic mice expressing the structural and nonstructural proteins of hepatitis C virus. Gastroenterology 2002, 122:352–365
8. Caronia S, Taylor K, Pagliaro L, Carr C, Palazzo U, Petrik J, O'Rahilly S, Shore S, Tom BD, Alexander GJ: Further evidence for an association between non-insulin-dependent diabetes mellitus and chronic hepatitis C virus infection. Hepatology 1999, 30:1059–1063
9. Mehta SH, Brancati FL, Sulkowski MS, Strathdee SA, Szklo M, Thomas DL: Prevalence of type 2 diabetes mellitus among persons with hepatitis C virus infection in the United States. Ann Intern Med 2000, 133:592–599
10. Choi J, Ou JH: Mechanisms of liver injury. III. Oxidative stress in the pathogenesis of hepatitis C virus. Am J Physiol Gastrointest Liver Physiol 2006, 290:G847–G851
11. Koike K, Miyoshi H: Oxidative stress and hepatitis C viral infection. Hepatol Res 2006, 34:65–76
12. Korenaga M, Wang T, Li Y, Showalter LA, Chan T, Sun J, Weinman SA: Hepatitis C virus core protein inhibits mitochondrial electron transport and increases reactive oxygen species (ROS) production. J Biol Chem 2005, 280:37481–37488
13. Moriya K, Nakagawa K, Santa T, Shintani Y, Fujie H, Miyoshi H, Tsutsumi T, Miyazawa T, Ishibashi K, Horie T, Imai K, Miyamura T, Kimura S, Koike K: Oxidative stress in the absence of inflammation in a mouse model for hepatitis C virus-associated hepatocarcinogenesis. Cancer Res 2001, 61:4365–4370
14. Moriya K, Fujie H, Shintani Y, Yotsuyanagi H, Tsutsumi T, Matsuura Y, Kimura S, Miyamura T, Koike K: The core protein of hepatitis C virus induces hepatocellular carcinoma in transgenic mice. Nat Med 1998, 4:1065–1067
15. Moriya K, Todoroki T, Tsutsumi T, Yotsuyanagi H, Tsutsumi T, Ishibashi K, Takayama T, Makuuchi M, Watanabe K, Miyamura T, Kimura S, Koike K: Increase in the concentration of carbon 18 monounsaturated fatty acids in the liver with hepatitis C: analysis in transgenic mice and humans. Biophys Biochem Res Commun 2001, 281:1207–1212
16. Shintani Y, Fujie H, Miyoshi H, Tsutsumi T, Kimura S, Moriya K, Koike K: Hepatitis C virus and diabetes: direct involvement of the virus in the development of insulin resistance. Gastroenterology 2004, 126:840–848
17. Piccoli C, Scrima R, Quarato G, D'Aprile A, Ripoli M, Lecce L, Boffoli D, Moradpour D, Capitanio N: Hepatitis C virus protein expression causes calcium-mediated mitochondrial bioenergetic dysfunction and nitro-oxidative stress. Hepatology 2007, 46:58–65
18. Cetinkale O, Konukoğlu D, Senel O, Kemerli GD, Yazar S: Modulating the functions of neutrophils and lipid peroxidation by FK506 in a rat model of thermal injury. Burns 1999, 25:105–112
19. Kaibori M, Inoue T, Tu W, Oda M, Kwon AH, Kamiyama Y, Okumura T: FK506, but not cyclosporin A, prevents mitochondrial dysfunction during hypoxia in rat hepatocytes. Life Sci 2001, 69:17–26
20. Keswani SC, Chander B, Hasan C, Griffin JW, McArthur JC, Hoke A: FK506 is neuroprotective in a model of antiretroviral toxic neuropathy. Ann Neurol 2003, 53:57–64
21. Kaymaz M, Emmez H, Bukan N, Dursun A, Kurt G, Paçsaoğlu H, Paçsaoğlu A: Effectiveness of FK506 on lipid peroxidation in the spinal cord following experimental traumatic injury. Spinal Cord 2005, 43:22–26
22. Ruggieri A, Murdolo M, Harada T, Miyamura T, Rapicetta M: Cell cycle perturbation in a human hepatoblastoma cell line constitutively expressing hepatitis C virus core protein. Arch Virol 2004, 149:61–74
23. Aizaki H, Harada T, Otsuka M, Seki N, Matsuda M, Li YW, Kawakami H, Matsuura Y, Miyamura T, Suzuki T: Expression profiling of liver cell lines expressing entire or parts of hepatitis C virus open reading frame. Hepatology 2002, 36:1431–1438
24. Todoroki T, Imai K, Matsumoto K, Kano S: Initial deactivation of Florisil adsorbent for column chromatographic separation of lipids. Analyst 1983, 108:1267–1269
25. Morrison WR, Smith LM: Preparation of fatty acid methyl esters and dimethylacetals from lipids with boron fluoride-methanol. J Lipid Res 1964, 5:600–608
26. Gelasco AK, Raymond JR: Indoxyl sulfate induces complex redox alterations in mesangial cells. Am J Physiol Renal Physiol 2006, 290:F1551–F1558
27. Williamson DH, Mellanby J, Krebs HA: Enzymic determination of D(−)-β-hydroxybutyric acid and acetoacetic acid in blood. Biochem J 1962, 82:90–96
28. Choi Y, Park Y, Pariza MW, Ntambi JM: Regulation of stearoyl-CoA desaturase activity by the *trans*-10,*cis*-12 isomer of conjugated linoleic acid in HepG2 cells. Biochem Biophys Res Commun 2001, 284:689–693
29. Williamson DH, Lund P, Krebs HA: The redox state of free nicotinamide-adenine dinucleotide in the cytoplasm and mitochondria of rat liver. Biochem J 1967, 103:514–527
30. Tsutsumi T, Suzuki T, Moriya K, Yotsuyanagi H, Shintani Y, Fujie H, Matsuura Y, Kimura S, Koike K, Miyamura T: Intrahepatic cytokine expression and AP-1 activation in mice transgenic for hepatitis C virus core protein. Virology 2002, 304:415–424
31. Moriishi K, Mochizuki R, Moriya K, Miyamoto H, Mori Y, Abe T, Murata S, Tanaka K, Suzuki T, Miyamura T, Koike K, Matsuura Y: Critical role of PA28γ in hepatitis C virus-associated steatogenesis and hepatocarcinogenesis. Proc Natl Acad Sci USA 2007, 104:1661–1666
32. Hoofnagle JH, Seeff LB: Peginterferon and ribavirin for chronic hepatitis C. N Engl J Med 2006, 355:2444–2451
33. Koike K: Antiviral treatment of hepatitis C: present status and future prospects. J Infect Chemother 2006, 12:227–232
34. Adinolfi LE, Gambardella M, Andreana A, Tripodi MF, Utili R, Ruggiero G: Steatosis accelerates the progression of liver damage of chronic hepatitis C patients and correlates with specific HCV genotype and visceral obesity. Hepatology 2001, 33:1358–1364
35. Patton HM, Patel K, Behling C, Tripodi MF, Utili R, Ruggiero G: The impact of steatosis on disease progression and early and sustained treatment response in chronic hepatitis C patients. J Hepatol 2004, 40:484–490
36. Hui JM, Sud A, Farrell GC, Bandara P, Byth K, Kench JG, McCaughan GW, George J: Insulin resistance is associated with chronic hepatitis C virus infection and fibrosis progression. Gastroenterology 2003, 125:1695–1704
37. Hickman IJ, Powell EE, Prins JB, Clouston AD, Ash S, Purdie DM, Jonsson JR: Insulin resistance is associated with chronic hepatitis C and virus infection fibrosis progression. J Hepatol 2003, 39:1042–1048
38. Han SY, Chang EJ, Choi HJ, Kwak CS, Suh SI, Bae JH, Park SB, Kim HC, Mun KC: Effect of tacrolimus on the production of oxygen free radicals in hepatic mitochondria. Transplant Proc 2006, 38:2242–2243
39. Staatz CE, Tett SE: Clinical pharmacokinetics and pharmacodynamics of tacrolimus in solid organ transplantation. Clin Pharmacokinet 2004, 43:623–653
40. Penfornis A, Kury-Paulin S: Immunosuppressive drug-induced diabetes. Diabetes Metab 2006, 32:539–546
41. van Hooff JP, Christiaans MH, van Duijnhoven EM: Evaluating mechanisms of post-transplant diabetes mellitus: Nephrol Dial Transplant 2004, 19(Suppl 6):vi8–vi12
42. Vigil SV, de Liz R, Medeiros YS, Fröde TS: Efficacy of tacrolimus in inhibiting inflammation caused by carrageenan in a murine model of air pouch. Transpl Immunol 2008, 19:25–29
43. Pereira R, Medeiros YS, Fröde TS: Antiinflammatory effects of tacrolimus in a mouse model of pleurisy. Transpl Immunol 2006, 16:105–111

JOURNAL OF VIROLOGY, May 2009, p. 5137–5147 Vol. 83, No. 10
0022-538X/09/$08.00+0 doi:10.1128/JVI.02179-08

Involvement of Creatine Kinase B in Hepatitis C Virus Genome Replication through Interaction with the Viral NS4A Protein[▽]

Hiromichi Hara,[1,2] Hideki Aizaki,[1] Mami Matsuda,[1] Fumiko Shinkai-Ouchi,[3] Yasushi Inoue,[1,4] Kyoko Murakami,[1] Ikuo Shoji,[1,5] Hayato Kawakami,[6] Yoshiharu Matsuura,[7] Michael M. C. Lai,[8] Tatsuo Miyamura,[1] Takaji Wakita,[1] and Tetsuro Suzuki[1]*

Department of Virology II[1] and Department of Biochemistry and Cell Biology,[3] National Institute of Infectious Diseases, Tokyo 162-8640, Japan; Department of Internal medicine, Division of Pulmonary Diseases, The Jikei University School of Medicine, Tokyo 105-8461, Japan[2]; Mita Hospital, International University of Health and Welfare, Tokyo 108-8329, Japan[4]; Division of Microbiology, Kobe University Graduate School of Medicine, Hyogo 650-0017, Japan[5]; Department of Anatomy, Kyorin University School of Medicine, Tokyo 181-8611, Japan[6]; Research Institute for Microbial Diseases, Osaka University, Osaka 565-0871, Japan[7]; and Department of Molecular Microbiology and Immunology, University of Southern California, Keck School of Medicine, Los Angeles, California 90033[8]

Received 15 October 2008/Accepted 20 February 2009

Persistent infection with hepatitis C virus (HCV) is a major cause of chronic liver diseases. The aim of this study was to identify host cell factor(s) participating in the HCV replication complex (RC) and to clarify the regulatory mechanisms of viral genome replication dependent on the host-derived factor(s) identified. By comparative proteome analysis of RC-rich membrane fractions and subsequent gene silencing mediated by RNA interference, we identified several candidates for RC components involved in HCV replication. We found that one of these candidates, creatine kinase B (CKB), a key ATP-generating enzyme that regulates ATP in subcellular compartments of nonmuscle cells, is important for efficient replication of the HCV genome and propagation of infectious virus. CKB interacts with HCV NS4A protein and forms a complex with NS3-4A, which possesses multiple enzyme activities. CKB upregulates both NS3-4A-mediated unwinding of RNA and DNA in vitro and replicase activity in permeabilized HCV replicating cells. Our results support a model in which recruitment of CKB to the HCV RC compartment, which has high and fluctuating energy demands, through its interaction with NS4A is important for efficient replication of the viral genome. The CKB-NS4A association is a potential target for the development of a new type of antiviral therapeutic strategy.

Hepatitis C virus (HCV) infection represents a significant global healthcare burden, and current estimates suggest that a minimum of 3% of the world's population is chronically infected (4, 19). The virus is responsible for many cases of severe chronic liver diseases, including cirrhosis and hepatocellular carcinoma (4, 16, 19). HCV is a positive-stranded RNA virus belonging to the family *Flaviviridae*. Its ~9.6-kb genome is translated into a single polypeptide of about 3,000 amino acids (aa), in which the nonstructural (NS) proteins NS2, NS3, NS4A, NS4B, NS5A, and NS5B reside in the C-terminal half region (6, 34, 44). NS4A, a small 7-kDa protein, functions as a cofactor for NS3 to enhance NS3 enzyme activities such as serine protease and helicase activities. The hydrophobic N-terminal region of NS4A, which is predicted to form a transmembrane α-helix, is responsible for membrane anchorage of the NS3-4A complex (8, 44, 50), and the central region of NS4A is important for the interaction with NS3 (10, 44). A recent study demonstrated the involvement of the C terminus of NS4A in the regulation of NS5A hyperphosphorylation and viral replication (28).

The development of HCV replicon technology several years ago accelerated research on viral RNA replication (7, 44). Furthermore, a robust cell culture system for propagation of infectious HCV particles was developed using a viral genome of HCV genotype 2a, JFH-1 strain, enabling us to study every process in the viral life cycle (27, 47, 54). RNA derived from genotype 1a, HCV H77, containing cell-culture adaptive mutations, also produces infectious viruses (52). Using these systems, it has been reported that the HCV genome replicates in a distinct, subcellular replication complex (RC) compartment, which includes NS3-5B and the viral RNA (2, 14, 33). The RC forms in a distinct compartment with high concentrations of viral and cellular components located on detergent-resistant membrane (DRM) structures, possibly a lipid-raft structure (2, 41), which may protect the RC from external proteases and nucleases. Almost all processes in viral replication are dependent on the host cell's machinery and involve intimate interaction between viral and host proteins. However, the functional roles of host factors interacting with the HCV RC in viral genome replication remain ambiguous.

To gain a better understanding of cellular factors that are components of the HCV RC and that function as regulators of viral replication, a comparative proteomic analysis of DRM fractions from HCV replicon and parental cells and subsequent RNA interference (RNAi) silencing of selected genes were performed. We identified creatine kinase B (CKB) as a key factor for the HCV genome replication. CKB catalyzes the reversible transfer of the phosphate group of phosphocreatine

* Corresponding author. Mailing address: Department of Virology II, National Institute of Infectious Diseases, 1-23-1 Toyama, Shinjuku-ku, Tokyo 162-8640, Japan. Phone: 81-3-5285-1111. Fax: 81-3-5285-1161. E-mail: tesuzuki@nih.go.jp.

▽ Published ahead of print on 4 March 2009.

(pCr) to ADP to yield ATP and creatine and is known to play important roles in local delivery and cellular compartmentalization of ATP (48, 51). The findings obtained here suggest that recruitment of CKB to the HCV RC, through CKB interaction with NS4A, is essential for maintenance or enhancement of viral replicase activity.

MATERIALS AND METHODS

Cell lines, antibodies, and reagents. Human hepatoma cell line Huh-7.5.1 (54) was kindly provided by Francis V. Chisari. Cell lines carrying subgenomic replicon RNAs, namely, SGR-N (41) and SGR-JFH1 (23), were derived from the HCV-N (17) and JFH-1 strains (24), respectively. Mouse monoclonal antibodies (MAbs) against HCV NS3 (Chemicon, Temecula, CA), NS4A (Santa Cruz Biotechnology, Inc., Santa Cruz, CA), NS5A (Biodesign, Saco, ME), NS5B (2), FLAG (M2; Sigma-Aldrich, St. Louis, MO), glyceraldehyde-3-phosphate dehydrogenase (GAPDH; Chemicon), and Flotillin-1 (BD Biosciences, San Jose, CA) and polyclonal antibodies (PAbs) against CKB (mouse [Abnova, Taipei, Taiwan], goat [Santa Cruz]), hemagglutinin (HA; Sigma-Aldrich), and FLAG (Sigma-Aldrich) were used. Cyclocreatine (Ccr; also known as 2-imino-1-imidazolidineacetic acid), pCr, and phosphopyruvic acid (pPy) were purchased from Sigma-Aldrich. Recombinant CKB and pyruvate kinase (PK) were obtained from Acris (Herfold, Germany) and Calbiochem (San Diego, CA), respectively.

Proteome analysis. RC-rich membrane fractions of cells were isolated as described previously (2, 41). Briefly, cells were lysed in hypotonic buffer. After removing the nuclei, supernatants were treated with 1% NP-40 for 60 min, mixed with 70% sucrose, overlaid with 55 and 10% sucrose, and centrifuged at 38,000 rpm for 14 h. Proteins from membrane fractions were purified by using a 2D Clean-Up kit (GE Healthcare, Tokyo, Japan), followed by labeling with fluorescent dyes: Cy5 for replicon cells, Cy3 for parental cells, and Cy2 for the protein standard containing equal amounts of both cell samples. Two-dimensional fluorescence difference gel electrophoresis (2D-DIGE) was performed using Immobiline DryStrip as the first-dimension gel and 12.5% polyacrylamide gel as the second-dimension gel. The 2D-DIGE images were analyzed quantitatively using the DeCyder software (GE Healthcare). Student *t* test was performed on differences between the tested samples using DeCyder biological variation analysis module. Samples were analyzed in triplicate. The protein spots of interest were excised from the gel, subjected to in-gel digestion using trypsin or lysyl endopeptidase and analyzed by liquid chromatography (MAGIC 2002 System; Michrom Bioresources, Auburn, CA) directly connected to electrospray ionization-ion trap mass spectrometry (LCQ-decaXP; Thermo Electron Corp., Iwakura, Japan). The results were subjected to database (NCBInr) search by Mascot server software (Matrix Science, Boston, MA) for peptide assignment.

Plasmids. A human CKB cDNA (43; kindly provided by Oriental Yeast Corp., Tokyo, Japan) was inserted into the EcoRI site of pCAGGS, yielding pCAGCKB. To generate expression plasmids for HA-tagged versions of wild-type and deletion mutated CKB, the corresponding DNA fragments were amplified by PCR, followed by introduction into the BglII site of pCAGGS. A fragment representing the inactive mutant CKB-C283S was synthesized by PCR mutagenesis. To generate FLAG-tagged NS protein expression plasmids, DNA fragments encoding either NS3, NS4A, NS4B, NS5A, or NS5B protein were amplified from HCV strains NIHJ1 (1) and JFH-1 (23) by PCR, followed by cloning into the EcoRI-EcoRV sites of pcDNA3-MEF (20). To generate an HA-tagged NS3 expression plasmid, a fragment encoding NS3 with the HA tag sequence at its N terminus was inserted into pCAGGS.

siRNA transfection. The small interfering RNAs (siRNAs) targeted to CKB (CKB-1 [5′-UAAGACCUUCCUGGUGUGGTT-3′] and CKB-2 [5′-CGUCAC CCUUGGUAGAGUUTT-3′]) and the scramble negative control siRNA to CKB-2 (5′-GGCGUACUAGCUUAUUCGCTT-3′) were purchased from Sigma. Cells in a 24-well plate were transfected with siRNA using HiPerFect transfection reagent (Qiagen, Tokyo, Japan) according to the manufacturer's instructions. The siRNA sequences for the other genes used in the siRNA screening are available upon request.

HCV infection. Culture media from Huh-7 cells transfected with in vitro-transcribed RNA corresponding to the full-length JFH-1 (47) was collected, concentrated, and used for the infection assay (3).

Quantification of HCV core protein and RNA. To estimate the levels of HCV core protein, aliquots of culture supernatants or of cell lysates were assayed by using HCV Core enzyme-linked immunosorbent assay kits (5). Total RNA was isolated from harvested cells using TRIzol (Invitrogen, Carlsbad, CA). Copy numbers of the viral RNA were determined by reverse transcription-PCR (RT-PCR) (2, 36, 46).

Immunoprecipitation, immunoblot analysis, and immunofluorescence microscopy. The analyses, as well as DNA transfection, were performed essentially as previously described (42). Cells were lysed in immunoprecipitation lysis buffer (50 mM Tris-HCl [pH 7.6], 150 mM NaCl, 1% sodium deoxycholate, 1% NP-40, 0.1% sodium dodecyl sulfate, 1 mM dithiothreitol, 1 mM calcium acetate). For immunoprecipitation, supernatants of cell lysates were precipitated with anti-FLAG antibody and protein A-Sepharose Fast Flow beads (GE healthcare). For immunofluorescence microscopy, anti-CKB goat PAb and anti-NS4A MAb as primary antibodies and Alexa Fluor 555-conjugated donkey anti-goat immunoglobulin G (Invitrogen) and Alexa Fluor 488-conjugated rabbit anti-mouse immunoglobulin G (Invitrogen) as secondary antibodies were used and observed under an LSM 510 confocal microscope (Carl Zeiss, Oberkochen, Germany).

Immunoelectron microscopy. Postembedding immunostaining using the colloidal gold-labeling method was performed as described previously (38). Cells were fixed in 4% paraformaldehyde–1% glutaraldehyde at 4°C for 1 h. After dehydration through a graded series of ethanol, cells were embedded in LR White (London Resin Company, London, United Kingdom) and sectioned. After blocking, section grids were incubated with a mixture of anti-NS4A and anti-CKB antibodies at 4°C overnight, followed by treatment with a mixture of 18-nm colloidal gold-conjugated donkey anti-mouse immunoglobulin G and 12-nm colloidal gold-conjugated donkey anti-goat immunoglobulin G antibodies (Jackson Immunoresearch, West Grove, PA) at 4°C overnight. The sections were stained with uranyl acetate and observed under a transmission electron microscope.

Measurement of CK activity and cellular ATP level. Cells were lysed with passive lysis buffer (Promega, Madison, WI), and CK activities were measured based on Oliver methods (40), in which the activity of converting creatine phosphate and ADP to creatine and ATP was measured. ATP levels in cell lysates were measured by using a CellTiter-Glo luminescent cell viability assay (Promega).

RNA replication assays in permeabilized replicon cells and in vitro. The RNA synthesis assay using permeabilized replicon cells was based on a previously described method (33). Briefly, SGR-JFH1 cells were treated with 5 μg of actinomycin D/ml for 2 h, followed by permeabilization with 50 μg of digitonin/ml for 5 min. The resulting mix was incubated with 500 μM concentrations of ATP, GTP, and CTP; 10 μCi of UTP ([α-^{32}P]UTP); 50 μg of actinomycin D/ml; and 5 mM pCr with or without 20 U of CKB/ml for 4 h at 27°C. RNA was extracted by using TRIzol and analyzed by 1% formaldehyde agarose gel electrophoresis. The cell-free RNA replication assay was performed as described previously (2).

In vitro helicase assays. Helicase activity on double-stranded RNA (dsRNA) was investigated as described previously (11) with some modifications. The 5′ end of the release strand was labeled with [γ-^{32}P]ATP using T4 polynucleotide kinase (Ambion). The dsRNA substrate was obtained by annealing the labeled RNA with a template strand RNA at a molar ratio of 1:1. The helicase assay mixture contained 5 nM dsRNA, helicase enzyme (80 nM NS3 or NS3-4A [kindly provided by R. De Francesco]), 6 mM ATP, in the presence or absence of 20 U of CKB/ml in an assay buffer (25 mM MOPS-NaOH [pH 7.0], 2.5 mM dithiothreitol, 100 μg of bovine serum albumin/ml, 3 mM $MgCl_2$, 5 mM pCr, 2.5 U of RNase inhibitor/ml). After the helicase reaction, samples were electrophoresed in a native 8% polyacrylamide gel and autoradiographed.

To determine the effect of PK/pPy system on the helicase activity, PK and pPy were used instead of CKB and pCr. Helicase activity on dsDNA was measured based on homogeneous time-resolved fluorescence quenching using a Trupoint helicase assay kit (Perkin-Elmer, Waltham, MA) according to the manufacturer's instructions.

In vitro protease assay. In vitro HCV protease activity of NS3-4A or NS3 was analyzed by using a SensoLyteHCV protease assay kit (AnaSpec, San Jose, CA) according to the manufacturer's instructions.

RESULTS

Identification of host factors involved in HCV RNA replication by comparative proteomic analysis of DRM fractions and RNAi silencing. To identify host proteins involved in the HCV RC, proteome profiles of the RC-rich membrane fraction in Huh-7 cells harboring subgenomic replicon RNA derived from genotype 1b, N isolate (SGR-N) were compared to those of parental cells by 2D-DIGE. We confirmed that the DRM fraction obtained from SGR-N cells is functionally active in a

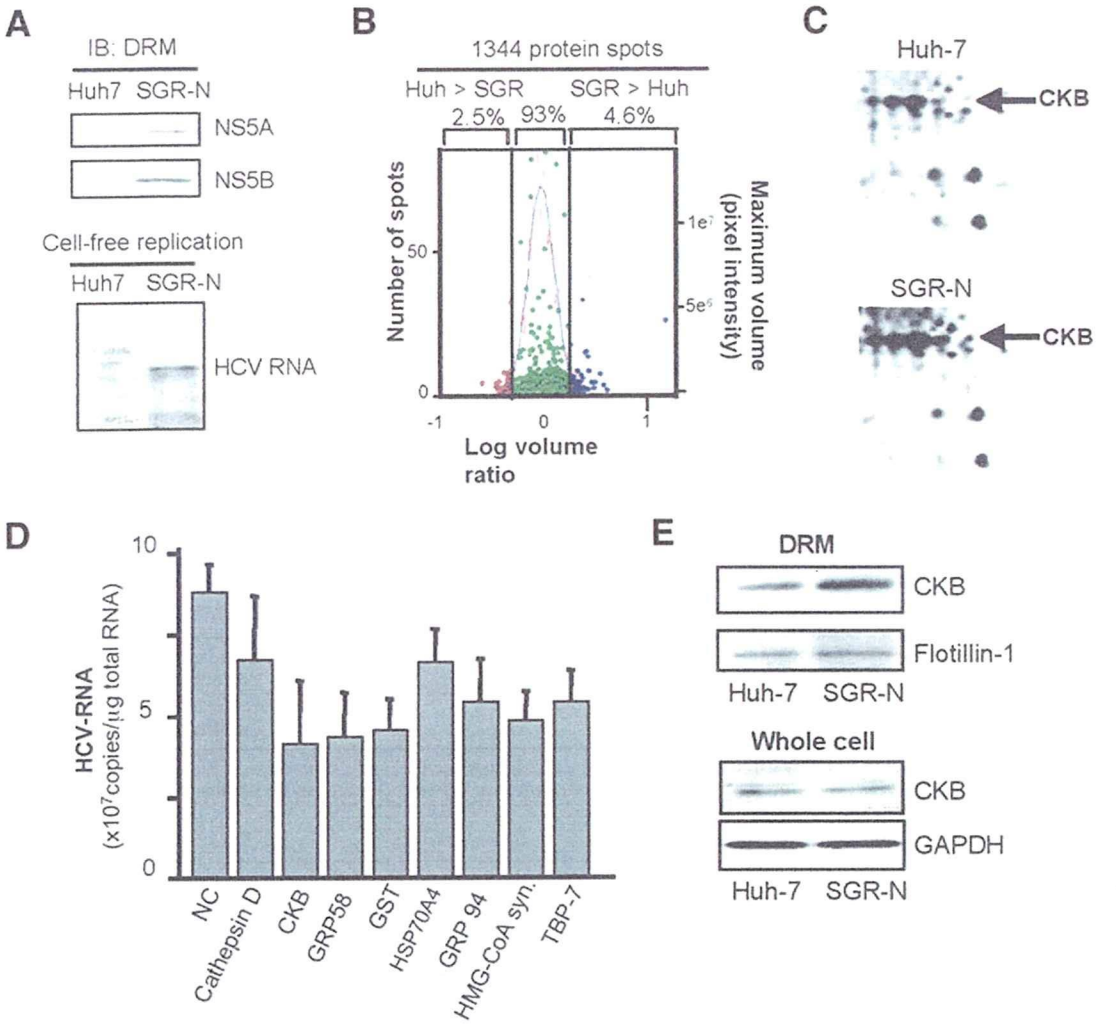

FIG. 1. Comparative proteomic analysis of DRM fractions and RNAi silencing. (A) Preparation of functionally active RC fraction for proteome analysis. DRM fractions obtained from SGR-N cells and parental Huh-7 cells were analyzed by immunoblotting with anti-NS5A and anti-NS5B antibodies (upper panel) and by the cell-free RNA replication assay (lower panel). (B) Histogram representation of proteins detected in 2D-DIGE. Images were analyzed quantitatively by the DeCyder software. The left and right *y* axis, respectively, indicate the spot frequency and the maximum volume of each spot, given against the log volume ratio (*x* axis). (C) Comparison of 2D-DIGE maps of proteins from DRM fractions of SGR-N cells and Huh-7 cells. Enlarged 2D-DIGE gel images of regions containing protein spots of CKB (arrows) are shown. (D) Effects of siRNAs of genes selected from comparative proteome analysis on HCV RNA replication. SGR-N cells were transfected with siRNA specific to cathepsin D, CKB (siCKB-1), GRP58, GST, Hsp70 protein 4, GRP94, HMG-coenzyme A synthase, or Tat binding protein 7 or with nontargeting (NC) siRNA. At 48 h posttransfection, total RNA was isolated and HCV RNA levels were assessed by real-time RT-PCR. (E) Enrichment of CKB in the DRM of HCV replicon cells. Equal amounts of DRM fractions from SGR-N and parental Huh-7 cells, or whole-cell lysates from both cells were analyzed by immunoblotting with antibodies against CKB, flotilin-1 or GAPDH.

cell-free replication assay (Fig. 1A). Three independent proteome experiments were performed for a reliable analysis of protein expression. Approximately 1,300 spots were resolved in each gel, and 4 to 5% of the protein spots represented a >2-fold increase in the membrane fraction of replicon cells in each experiment (Fig. 1B). The protein spots that exhibited high reproducibility (an example shown in Fig. 1C) were excised, digested by trypsin or lysyl endopeptidase, and analyzed by mass spectrometry, which identified the corresponding proteins in 27 cases (Table 1). Among the proteins implicated in a variety of functional categories, 10 were involved in protein folding, mainly as chaperones, 7 were metabolic and biosynthesis enzymes including proteins for redox regulation or energy pathways, 3 were involved in cytoskeleton organization, and 3 proteins were related to cellular processes, mainly proteolysis pathways. The viral NS proteins identified as differentially expressed proteins in the analysis were not listed.

In order to identify host factors involved in HCV replication, we examined the effects on viral RNA replication of transfection of SGR-N cells with siRNAs against genes encoding nine proteins belonging to diverse classes of biological functions (Table 1). Each siRNA reduced the HCV RNA level to 47 to 76% of the level of the siRNA control (Fig. 1D). None of the siRNAs tested exhibited considerable cytotoxicity against the replicon cells, ruling out overt toxicity as a mechanism for inhibition of viral RNA replication. Among the candidate

TABLE 1. Selected proteins that reproducibly increased in the DRM fraction of SGR-N cells[a]

Avg ratio	*P* (Student *t* test)	Coverage (%)	Protein name	Molecular function	GI no.
5.56	0.04	27	GRP94	Protein folding	15010550
4.99	0.07	47	Hsp60	Protein folding	6996447
3.73	0.07	6	tRNA guanine transglycosylase	Metabolism	30583205
3.56	0.06	23	KIAA0088	Unknown	577295
3.32	0.07	4	Thioredoxin-related protein	Unknown	20067392
3.32	0.13	12	Tat binding protein 1 (TBP-1)	Cellular processes	20532406
3.06	0.14	22	Aldehyde dehydrogenase 1	Metabolism	2183299
3.06	0.14	14	Chaperonin TRiC/CCT, subunit 2	Protein folding	54696794
2.96	0.04	14	Heat shock 70-kDa protein 4 (HSPA4)	Protein folding	6226869
2.96	0.04	29	GRP58	Metabolism/protein folding	2245365
2.94	0.01	37	Mutant β-actin	Cytoskeleton organization	28336
2.65	0.17	33	Glutathione S-transferase (GST)	Catalytic activity	2204207
2.53	0.04	37	Keratin 19	Cytoskeleton organization	6729681
2.46	0.08	6	Heterogeneous nuclear ribonucleoprotein K	Nucleic acid modification	460789
2.45	0.001	13	HMG-coenzyme A synthase	Metabolism	30009
2.4	0.02	31	CKB	Energy pathway/metabolism	180570
2.4	0.02	11	Cathepsin D	Cellular processes	30582659
2.4	0.02	11	C8orf2	Unknown	37181322
2.36	0.1	38	Tropomyosin 4-anaplastic lymphoma kinase fusion protein	Cytoskeleton organization	14010354
2.36	0.1	6	Calreticulin	Protein folding	30583735
2.33	0.01	29	Quinolinate phosphoribosyltransferase	Metabolism	30583301
2.29	0.04	25	Protein disulfide isomerase-related protein 5	Protein folding	1710248
2.29	0.04	16	Tat binding protein 7 (TBP-7)	Cellular processes	263099
2.05	0.11	24	Calumenin	Metabolism	2809324
2.05	0.12	10	TRiC/CCT, subunit 5	Protein folding	24307939
2.03	0.07	20	Hsp90 beta	Protein folding	34304590
2.01	0.07	10	TRiC/CCT, subunit 1	Protein folding	36796

[a] The spectra obtained by tandem mass spectrometry were collected using data-dependent mode, and the results were subjected to database (NCBInr) search by Mascot server software (Matrix Science, London, United Kingdom) for peptide assignment. Coverage, the ratio of the portion of protein sequence covered by matched peptides to the whole protein sequence. GI no., GenInfo identifier number.

genes examined, we observed a reproducible inhibition of HCV RNA replication by two independent siRNAs targeting CKB (see below).

CKB participates in HCV RNA replication and the propagation of infectious virus. CKB is a brain-type creatine kinase isoenzyme and is also detected in a variety of other tissues, including human liver (32). Steady-state levels of CKB in the DRM fraction, as well as in whole-cell lysate of SGR-N cells were compared to those from parental cells by Western blotting. The CKB level in the DRM fraction of replicon cells was higher than that in parental cells (Fig. 1E), confirming the results of the proteome analysis described above. In contrast, the CKB level in whole cells was similar in both cells (Fig. 1E). These results suggest participation of posttranslational modification, such as translocation to the DRM fraction, of CKB in replicon cells.

Figure 2A shows the inhibitory effect on HCV RNA replication of CKB siRNA; siCKB-2, the sequence of which does not overlap with the sequence of siCKB-1 used in the above siRNA screening (Fig. 1D). Transfection with siCKB-2 effectively decreased the cellular level of CKB enzymatic activity (data not shown), as well as the abundance of CKB protein (Fig. 2A), and resulted in 60% reduction in the viral RNA level in SGR-N cells compared to the cells treated with control siRNA. This inhibitory effect of siRNA on HCV RNA abundance was also observed in JFH-1-derived subgenomic replicon (SGR-JFH1) cells. The viral RNA level in the cells transfected with siCKB-2 decreased by 50% compared to the control (Fig. 2A). We also tested the CKB mutant, CKB-C283S, in which Cys at aa 283, near the catalytic site, has been replaced with Ser (Fig. 3A) and which is known to be enzymatically inactive and to work in a dominant-negative manner (22, 29). As expected, overexpression of CKB-C283S resulted in a reduction in HCV RNA replication in SGR-N cells (Fig. 2B). We obtained a similar result in SGR-JFH1 cells, as described below (Fig. 3E).

To further examine the involvement of CKB in HCV RNA replication, we tested the effect of Ccr, a substrate analogue and possible inhibitor for CK in either SGR-N, SGR-JFH1 (Fig. 2C), or Huh7 cells transiently replicating luciferase-subgenomic replicon (data not shown). We found dose-dependent inhibition of HCV RNA replication but no observed effect on total cellular levels of protein and ATP (Fig. 2D) in the replicon setting used.

We next examined whether the knockdown of CKB or treatment with Ccr would abrogate the production of HCVcc. At 72 h posttransfection with siCKB-2, the HCV core level in cells infected with HCVcc was significantly reduced (Fig. 2E). Treatment of the infected cells with Ccr at various concentrations also reduced the intracellular and supernatant core level and subsequently decreased HCVcc production (Fig. 2F). These results demonstrate that suppression of the HCV RNA replication by the siRNA-mediated knockdown of CKB or treatment with CKB inhibitor leads to reduction of the production of infectious virus.

CKB interacts with HCV NS4A. Having established a role for CKB in HCV RNA replication, we then tried to determine to how CKB influences the HCV life cycle. It has been re-